A

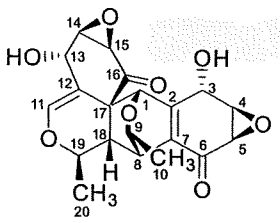

Epoxyquinol B

B

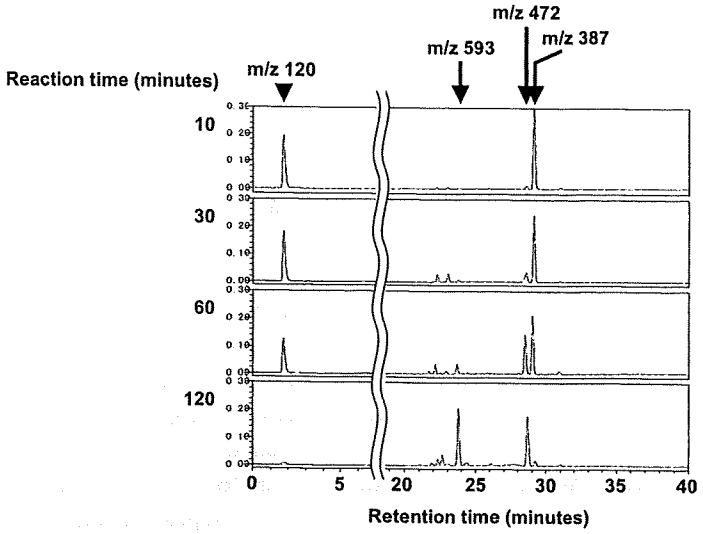

Fig. 1 HPLC and LC/MS analysis of reaction products between EPQB and *L*-cysteine.

(A) Structure of Epoxyquinol B (EPQB). (B) HPLC and LC/MS analyses of reaction of EPQB and cysteine. 10 mM EPQB and 100 mM *L*-cysteine were incubated in water for 10, 30, 60, and 120 minutes at 4°C. The samples were separated by XTerra MSC18 column. HPLC and LC/MS systems were carried out by Allians 2695 Separation Module (Waters) and Q TRAP LC/MS/MS System (Applied Biosystems) with XTerra MSC18 column by using a gradients of 0.05% formic acid and acetonitrile (2~100%).

determined as $[EPQB+2Cys\text{-}2H_2O-H]^-$ (Rt: 23.8 minutes, *m/z*: 593.0) and $[EPQB+1Cys\text{-}2H_2O-H]^-$ (Rt: 28.7 minutes, *m/z*: 472.0), respectively. These results suggest that one EPQB molecule is sequentially bound to two cysteine molecules through two of its reactive sites. The UV spectra of EPQB, $EPQB+1Cys\text{-}2H_2O$, and $EPQB+2Cys\text{-}2H_2O$ show absorption maxima at 237, 225, and 220 nm, respectively (data not shown), indicating that these compounds containing the same chromophore derived from a α,β-unsaturated ketone. Therefore, it was strongly suggested that this conjugated system retained in the molecules of two reaction products and thus the reaction sites on EPQB are two epoxides. To confirm this possibility, we analyzed the structures of two reaction products. EPQB was incubated with *L*-cysteine for 1 and 4 hours, by ^{1}H-NMR. Since it was difficult to isolate enough amount of these products for NMR analysis, the reaction mixture was lyophilized, dissolved again in methanol-d_4 and prepared for the measurement of ^{1}H and DQF-COSY spectra by a Jeol JNM ECP-500 NMR spectrometer. The ^{1}H-NMR data revealed that the ratio of integration value between methyl doublets of EPQB (1.24 ppm, J=6.4 Hz), and each product (product 1: 1.26 ppm, J=6.4 Hz, and product 2: 1.28 ppm, J=6.4 Hz) was two to one. As the ^{1}H signal derived from 11-H (6.4 ppm, s) was still observed in the ^{1}H-NMR spectra of both products, the addition site of cysteine molecule was supposed to be on two epoxide part of EPQB. (The numbering of both products was temporarily assigned on the basis of the corresponding carbon atoms of EPQB.) We focused on the analysis of the ^{1}H chemical shifts of epoxide parts in both reaction products. The assignments of 13-H, 14-H and 15-H were difficult because of overlapping with

the background signals from the reaction mixture. On the other hand, the signals of 3-H, 4-H and 5-H of products were observed separately. The signal of 4-H of EPQB (3.80 ppm, dd, J=1.4, 3.7 Hz) shifted to high magnetic field (product 1: 3.63 ppm, dd, J=1.8, 3.2 Hz, product 2: 3.62 ppm, dd, J=1.8, 2.8 Hz), because of the formation of the C-S bond in adducts instead of the C-O bond in EPQB. The cross peak was due to the protons attached to the carbon atoms originated from C4 and C5 of EPQB. It was clearly observed in the DQF-COSY spectrum. Furthermore, the stereo-structure of the products was investigated by the Dreiding model. It was considered that the six membered ring of the products has 3-α-OH, 4-β-H, 5-β-OH and α,β-unsaturated ketone system, because of the subsequent ring opening of epoxide accompanied with the inversion of 4-H. The dihedral angle of 50~55° between 3-H and 4-H and 110~115° between 4-H and 5-H were correlated to J values as given in the NMR spectrum by the Karplus's correlation between dihedral angle and J values [5]. These results suggested that the initial binding site of *L*-cysteine in EPQB was the C-4 position. The analyses of LC/MS, UV, and NMR data indicated that one molecule of EPQB binds to two molecules of *L*-cysteine through its opening of the two epoxides.

When EPQB was treated with recombinant VEGFR2 kinase protein, we noticed that several ladder-like hypershifted bands appeared with EPQB-dependent manner (Fig. 2A). Since it was previously shown that one EPQB covalently binds to two cysteines, we anticipated that EPQB crosslinked the binding proteins through the cysteine residues. To investigate this possibility, we used cysteine/serine-mutated Vh1 related phosphatase (VHR) proteins [6, 7] as a model protein. VHR protein contains only four cysteine residues; Cys22, Cys30, Cys124, and Cys171. Therefore, we made two mutant VHR proteins, 3S and 4S; in these mutant proteins, three of the cysteines (C22/30/124) and all of the cysteines (C22/30/124/171) on VHR were replaced with serines, respectively. Wild type (WT) or each cysteine/serine mutant VHR (3S and 4S) were incubated with 10 mM EPQB in water and VHR buffer (50 mM Tris-HCl (pH 7.5) and 1.0 mM EDTA) for 1 hour. The samples were separated with SDS-PAGE and the VHR proteins were detected by western blotting analysis. As shown in Fig. 2B, ladder-like hypershifted bands were observed in EPQB-treated WT VHR proteins. On the contrary, only dimerized band of VHR was appeared when EPQB was treated with 3S mutant VHR protein which contains only one cysteine. Furthermore, no additional band was observed when EPQB was treated with 4S mutant VHR protein. The data shown in Fig. 2B was obtained in the water condition to correlate with the LC/MS

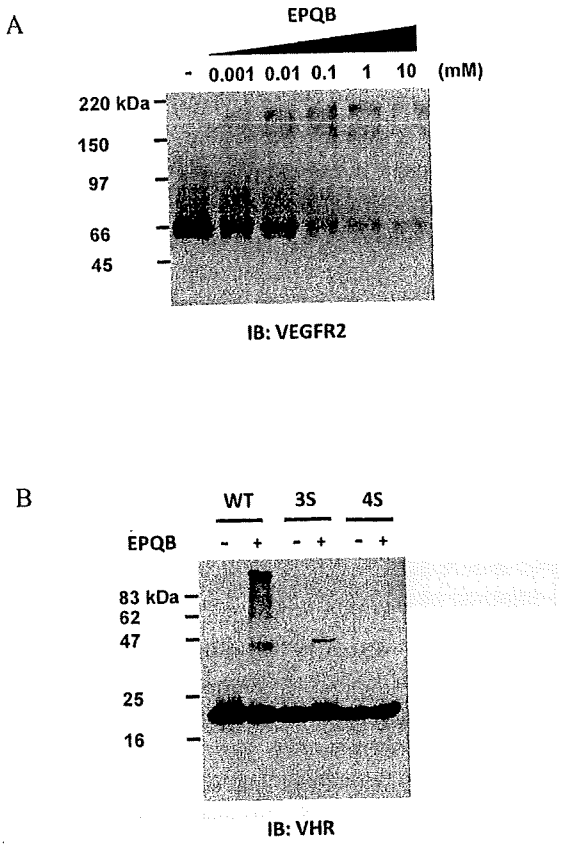

Fig. 2 EPQB crosslinks VHR protein through the binding with cysteine residues.

(A) The appearance of a ladder-like hypershifted bands containing recombinant VEGFR2 kinase protein by EPQB treatment. Recombinant VEGFR2 kinase protein (66 kDa) was treated with 0.001, 0.01, 0.1, 1, and 10 mM EPQB for 2 hours *in vitro*. These samples were analyzed by Western blotting. (B) Crosslinking assay of EPQB. Wild type (WT) or cysteine/serine mutant (3S and 4S) VHR (400 ng) were incubated with 10 mM EPQB in water for 1 hour. The proteins were separated with SDS-PAGE and VHR proteins (21 kDa) were detected by Western blotting.

experiment condition. In fact, there were no differences in the crosslinking pattern between the water and the VHR buffer conditions (data not shown). These results strongly suggest that EPQB crosslinked proteins through the cysteine residues on its target protein.

Recently, there have been a few reports on small-molecule ligands containing two protein-binding surfaces. These ligands modulate a number of cellular processes especially signal transduction pathways. FK1012A, which is a dimer of FK506, is developed as a pharmacological mediator. It induced dimerization of the FK506-binding protein and consequently initiated the signaling cascade [8~10]. Furthermore, Guido L. *et al.* suggested that helenalin, a sesquiterpene lactone, crosslinks protein

through the cysteine residues of NF-κB [11]. Since the active site of NF-κB contains cysteine residues, the binding and crosslinking by helenalin may affect the signaling pathway. Our results showed that one EPQB also binds to two cysteine residues in its binding protein(s), and suggests that EPQB may consequently inhibit angiogenesis signal transductions through inter/intramolecular crosslinking of the target proteins.

Acknowledgment This study was supported in part by Junior Research Associate, Grants for Basic Research (Chemical Biology Project) from RIKEN, and a Grant-in-Aid from the Ministry of Education, Culture, Sports, Science, and Technology of Japan. We thank Naoki Kanoh (Tohoku University) for technical advice and useful discussion.

References

1. Mateo C, Abian O, Fernández-Lorente G, Pedroche J, Fernández-Lafuente R, Guisan JM, Tam A, Daminati M. Epoxy sepabeads: a novel epoxy support for stabilization of industrial enzymes *via* very intense multipoint covalent attachment. Biotechnol Prog 18: 629–634 (2002)
2. Kakeya H, Onose R, Yoshida A, Koshino H, Osada H. Epoxyquinol B, a fungal metabolite with a potent antiangiogenic activity. J Antibiot 55: 829–831 (2002)
3. Kakeya H, Onose R, Koshino H, Yoshida A, Kobayashi K, Kageyama S, Osada H. Epoxyquinol A, a highly functionalized pentaketide dimer with antiangiogenic activity isolated from fungal metabolites. J Am Chem Soc 124: 3496–3497 (2004)
4. Kamiyama H, Kakeya H, Usui T, Nishikawa K, Shoji M, Hayashi Y, Osada H. Epoxyquinol B shows antiangiogenic and antitumor effects by inhibiting VEGFR2, EGFR, FGFR, and PDGFR. Oncology Res (in press)
5. Karplus M. Contact electron-spin coupling of nuclear magnetic moments. J Chem Phys 30: 11–15 (1959)
6. Ishibashi T, Bottaro DP, Chan A, Miki T, Aaronson SA. Expression cloning of a human dual-specificity phosphatase. Proc Natl Acad Sci USA 89: 12170–12174 (1992)
7. Ueda K, Usui T, Nakayama H, Ueki M, Takio K, Ubukata M, Osada H. 4-Isoavenaciolide covalently binds and inhibits VHR, a dual-specificity phosphatase. FEBS Lett 525: 48–52 (2002)
8. Spencer DM, Wandless TJ, Schreiber SL, Crabtree GR. Controlling signal transduction with synthetic ligands. Science 262: 1019–1024 (1993)
9. Diver ST, Schreiber SL. Single-step synthesis of cell-permeable protein dimerizers that activate signal transduction and gene expression. J Am Chem Soc 119: 5106–5109 (1997)
10. Blau CA, Peterson KR, Drachman JG, Spencer D. A proliferation switch for genetically modified cells. Proc Natl Acad Sci USA 94: 3076–3081 (1997)
11. Guido L, Knorre A, Schmidt TJ, Pahl HL, Merfort I. The anti-inflammatory sesquiterpene lactone helenalin inhibits the transcription factor NF-κB by directly targeting p65. J Biol Chem 273: 33508–33516 (1998)

Natural Product Synthesis

DOI: 10.1002/anie.200802079

The Asymmetric Total Synthesis of (+)-Cytotrienin A, an Ansamycin-Type Anticancer Drug**

Yujiro Hayashi, Mitsuru Shoji, Hayato Ishikawa, Junichiro Yamaguchi, Tomohiro Tamura, Hiroki Imai, Yosuke Nishigaya, Kenichi Takabe, Hideaki Kakeya, and Hiroyuki Osada*

Cytotrienin A (**1**) is a microbial antitumor secondary metabolite that was isolated from the fermentation broth of *Streptomyces sp.* RK95-74 from soil.[1] It possesses an

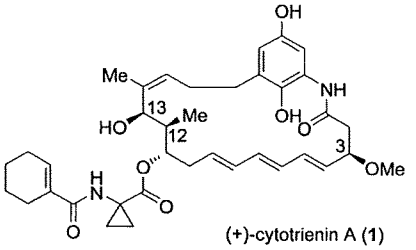

(+)-cytotrienin A (**1**)

E,E,E-triene motif within a 21-membered cyclic lactam, which also contains four chiral centers. These are common structural features of the ansamycin class of natural products, which include the mycotrienins (or ansatrienins),[2] trienomycins,[2c,3] thiazinotrienomycins,[4] and trierixin.[5] Cytotrienin A, with its unusual aminocyclopropane carboxylic acid side chain, exhibits potent apoptosis-inducing activity on HL-60 cells with an ED_{50} value of 7.7 nM. To facilitate elucidation of its mechanism of action, the development of a method for the total synthesis and derivatization of cytotrienin A is highly desirable. The research groups of Smith and Panek have accomplished the total synthesis of other members of this class of natural products, including trienomycins A and F,[6] mycotrienin A,[7] and thiazinotrienomycin E.[8] Although the macrocyclic core of cytotrienin A has been synthesized in its protected form by Panek et al.[9] and Kirschning et al.,[10] the total synthesis of cytotrienin A, with the side chain attached, has not been reported. The relative and absolute stereochemistry has not been confirmed, but has been assigned based on analogous mycotrienin natural products. Herein we report the first total synthesis of the naturally occurring enantiomer of cytotrienin A, which confirms its relative and absolute stereochemistry.

We envisioned installing the side chain midway through the synthesis and constructing the triene unit at a late stage by ring-closing metathesis (RCM).[11] We reasoned that introduction of the bulky side chain after formation of the macrocyclic core would be difficult, and also, a long sequence of reactions after the construction of the labile triene unit would be avoided. Other noteworthy features of our approach are the use of novel organocatalyzed and proline-mediated enantioselective reactions, both of which have been developed by our research group.[12] Specifically, we planned to form two (C11 and C12) of the three contiguous chiral centers with an aldol reaction by using an organocatalyst, and to control the configuration at C3 by using proline-mediated α-aminoxylation.

The synthesis started with an organocatalyzed aldol reaction which was found to be problematic. The original procedure[13] which used proline was not practical for large-scale synthesis owing to the excess amount of furfural required (10 equivalents), low yield, and low diastereoselectivity [Eq. (1)]. After some experimentation, diol **2** was obtained in good yield and with good d.e. when the reaction was conducted without solvent using surfactant-proline con-

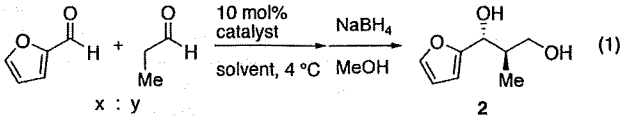

(1)

proline x/y = 10:1 DMF 32 h 10% *anti/syn* = 1:1

cat. **33** x/y = 1:5 neat 48 h 77% *anti/syn* = 6.2:1, 96% *ee*

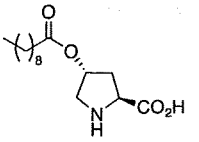

33

[*] Prof. Dr. Y. Hayashi, Dr. M. Shoji,[+] Dr. H. Ishikawa, J. Yamaguchi, T. Tamura, H. Imai, Y. Nishigaya, K. Takabe
Department of Industrial Chemistry, Faculty of Engineering
Tokyo University of Science, Kagurazaka, Shinjuku-ku, Tokyo 162-8601 (Japan)
Fax: (+81) 3-5261-4631
E-mail: hayashi@ci.kagu.tus.ac.jp
Homepage: http://www.ci.kagu.tus.ac.jp/lab/org-chem1/
Prof. Dr. H. Kakeya
Graduate School of Pharmaceutical Sciences
Kyoto University, Sakyo-ku, Kyoto-city, Kyoto 606-8501 (Japan)
Prof. Dr. H. Osada
Antibiotics Laboratory
RIKEN Discovery Research Institute
Wako, Saitama 351-0198 (Japan)
[+] Present address:
Department of Chemistry, Graduate School of Science
Tohoku University, Sendai 980-8578 (Japan)

[**] This work was supported by a Grant-in-Aid for Creative Scientific Research from The Ministry of Education, Culture, Sports, Science, and Technology (MEXT).

Supporting information for this article is available on the WWW under http://dx.doi.org/10.1002/anie.200802079.

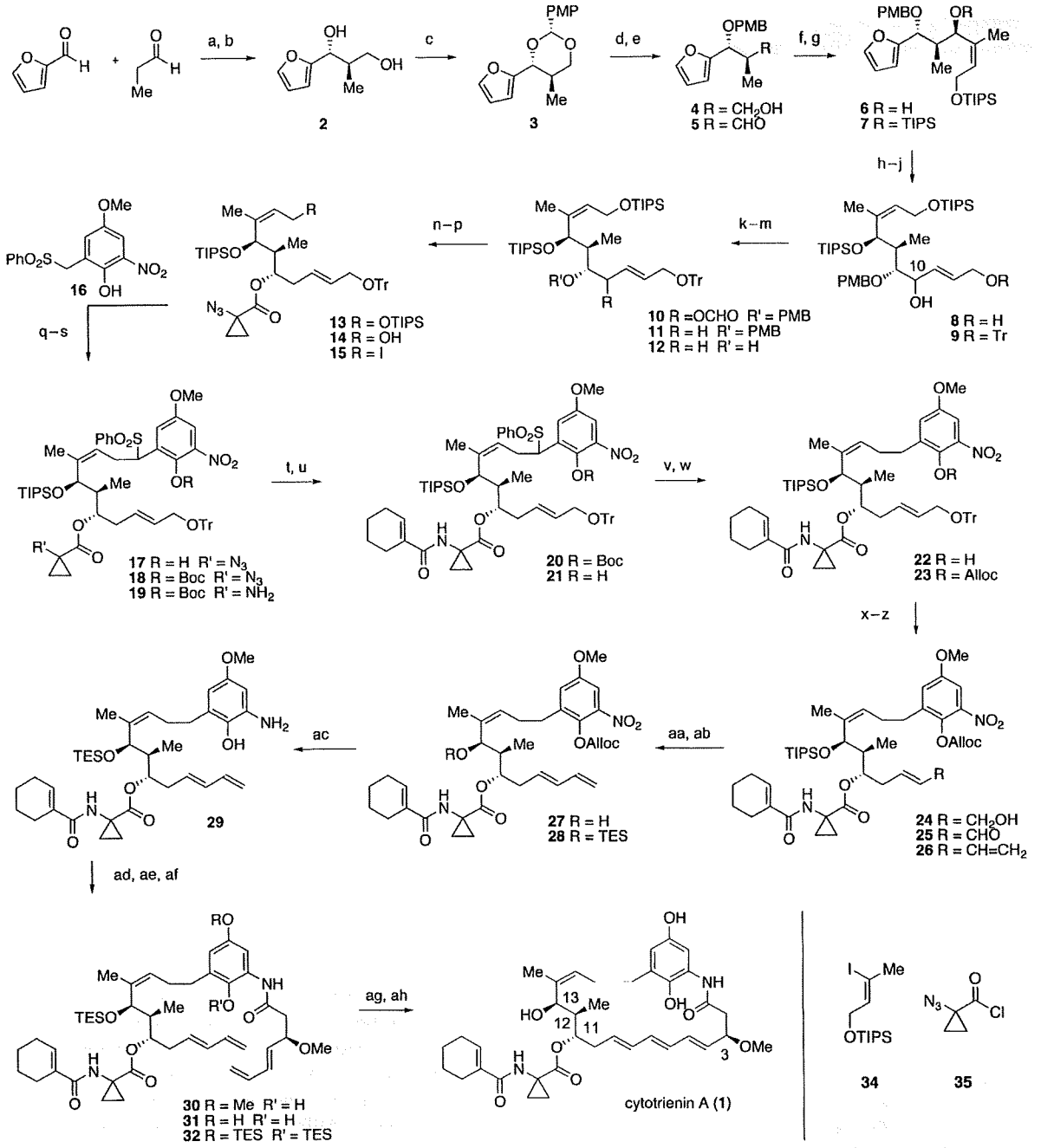

Scheme 1. Reagents and conditions: a) **33**, 4 °C, 48 h; b) $NaBH_4$, MeOH, 0 °C, 1 h (77%, 96% *ee*, *anti*:*syn* 6.2:1); c) *p*-MeOPhCH$(OMe)_2$, PPTS, benzene, 80 °C, 1 h (64%, >99% *ee* after recrystallization); d) DIBAL-H, Et_2O, −78 °C to −10 °C, 128 h [80% (92% brsm)]; e) SO_3·py, DMSO, Et_3N, CH_2Cl_2, 0 °C, 45 min (quant.); f) **34**, *t*BuLi, THF, −78 °C, 1 h; Me_2Zn, 0 °C, 20 min; then **5** at −78 °C; −35 °C, 3 h (79%); g) TIPSOTf, 2,6-lutidine, CH_2Cl_2, 0 °C, 23 h (99%); h) O_2, Rose Bengal, EtCN, *hν*, −78 °C, 8 h; Me_2S, −20 °C, 15 h; DABCO, −20 °C, 2 h; i) $NaBH_4$, $CeCl_3·7H_2O$, EtOH, 0 °C, 20 min (81% from **7**); j) TrCl, Et_3N, CH_2Cl_2, 23 °C, 3 h (93%); k) 1*H*-benzotriazole-1-carbaldehyde, DMAP, CH_2Cl_2, 23 °C, 4 h (quant.); l) $[Pd_2(dba)_3]·CHCl_3$, nBu_3P, HCO_2NH_4, 1,4-dioxane, 23 °C, 67 h (76%); m) DDQ, CH_2Cl_2/pH 7 phosphate buffer, 0 °C, 4 h (96%); n) **35**, DMAP, Et_3N, 0 °C, 20 min (98%); o) py(HF)$_x$, THF, 23 °C, 17 h (84%); p) I_2, Ph_3P, imidazole, benzene, 23 °C, 30 min; q) **16**, LHMDS, THF, −90 °C, 40 min; then **15** at −90 °C; −65 °C, 18 h (78% from **14**); r) $(Boc)_2O$, DMAP, CH_2Cl_2, 23 °C, 30 min (96%); s) 1,3-propanedithiol, Et_3N, MeOH, 23 °C, 18 h (87%); t) 1-cyclohexenecarboxylic acid, EDCI, DMAP, CH_2Cl_2, 23 °C, 21 h (78%); u) pyrrolidine, CH_2Cl_2, 23 °C, 5 h; v) $NaBH_4$, EtOH, 50 °C, 21 h (57% from **20**); w) AllocCl, Et_3N, CH_2Cl_2, 23 °C, 40 min; x) TsOH·H_2O, MeOH, 23 °C, 1 h (94% from **22**); y) MnO_2, CH_2Cl_2, 23 °C, 40 min; z) $[Ph_3P^+CH_3]I^-$, *t*BuOK, THF, 0 °C, 30 min (74% from **24**); aa) 46% HF, MeCN, 23 °C, 16 h [68% (91% brsm)]; ab) TESOTf, iPr_2EtN, CH_2Cl_2, 23 °C, 30 min (99%); ac) $NaBH_4$, S_8, THF, 50 °C, 2.5 h; ad) **42**, BOP-Cl, iPr_2EtN, toluene, 23 °C, 8 h; K_2CO_3, MeOH, 23 °C, 10 min (79% from **28**); ae) MnO_2, CH_2Cl_2, 23 °C, 5 min; $NaBH_4$, MeOH, 0 °C; af) 4-triethylsiloxy-3-penten-2-one, DMF, 23 °C to 50 °C, 9 h (77% from **30**); ag) Grubbs I catalyst (40 mol%), CH_2Cl_2, 23 °C, 71 h [39% (51% brsm)]; ah) Amberlyst 15, THF/H_2O (10:1), 23 °C, 47 h (95%). Definitions of acronyms given in reference [28].

jugated catalyst **33**.[14] This catalyst was developed by us for aldol reactions in the presence of water. As this reaction proceeds without solvent, scale-up and purification are straightforward. Diol **2** was treated with *p*-anisaldehyde dimethyl acetal in the presence of PPTS to provide **3**, which was isolated in diastereomerically and optically pure form (>99% *ee*) after recrystallization (and without the need for column chromatography; Scheme 1).

Reduction of **3** with DIBAL-H gave primary alcohol **4** in 80% yield (92% yield based on recovered starting material (brsm)). Alcohol **4** was oxidized to aldehyde **5** quantitatively. The reaction of **5** with vinyl zincate,[15] prepared from vinyl iodide **34** with *t*BuLi and Me_2Zn, proceeded in a highly diastereoselective manner to afford **6** as a single isomer in 79% yield. Notably, other vinyl metals gave low diastereoselectivities.[16] The secondary hydroxy group of **6** was protected with the TIPS group. The furan ring was cleaved by oxidation with O_2 under irradiation conditions in the presence of Rose Bengal.[17] Subsequent *cis/trans* isomerization using DABCO, followed by Luche reduction[18] gave diol **8** as a mixture of diastereomers at C10 in 81% yield (over 3 steps). The primary hydroxy group of **8** was protected as the trityl ether. The free hydroxy group of **9** was converted into formate ester **10**, which was removed by reduction using a palladium–PBu_3 complex with the protocol developed by Tsuji and co-workers [19] to provide **11** as a single isomer without positional or *E*/*Z* isomerization. Removal of the PMB group followed by reaction with acid chloride **35**[20] gave ester **13**. Selective removal of the TIPS group gave primary alcohol **14**, which was transformed into iodide **15** with PPh_3 and I_2. Coupling of fragment **15** and sulfone **16** was successfully performed by the lithiation of hydroxysulfone **16** with LHMDS, followed by alkylation using **15** to afford **17** in 78% yield (over 2 steps). After protection of the phenol of **17** as its Boc derivative, the azide moiety was reduced to an amine with 1,3-propanedithiol,[21] and the amide bond with cyclohexenyl carboxylic acid was constructed to provide **20** in good yield. This completed installation of the side chain.

Carrying out desulfonylation without affecting the nitro group was difficult. After experimentation, a novel method was developed which consisted of removal of the Boc group with pyrrolidine[22] followed by treatment of phenol **21** with $NaBH_4$. This method provided **22** in 57% yield (over 2 steps) through a retro-Michael reaction with SO_2Ph, probably involving *o*-quinonemethide, followed by reduction with $NaBH_4$. The phenol was protected as its Alloc derivative and removal of the Tr group gave alcohol **24** in 94% yield (over 2 steps). Oxidation of **24** with MnO_2, followed by a Wittig reaction gave diene **26** in 74% yield (over 2 steps). As we could not remove the TIPS group after construction of the triene moiety, this protecting group was replaced with the easily removable TES group at this stage. Treatment with HF provided **27** in 91% yield (brsm), then reaction with TESOTf afforded **28** quantitatively. The nitro group was reduced with $NaBH_2S_3$[23] and was accompanied by removal the Alloc group to provide **29**. The amine **29** was treated with carboxylic acid **42** (vide infra) in the presence of BOP-Cl to afford **30** in 79% yield (over 2 steps).

Carboxylic acid **42** was synthesized as shown in Scheme 2. Proline-mediated α-aminoxylation[24] of aldehyde **36** proceeded efficiently to provide **37**. Under Horner–Emmons reaction conditions, a crude sample of **37** was converted into

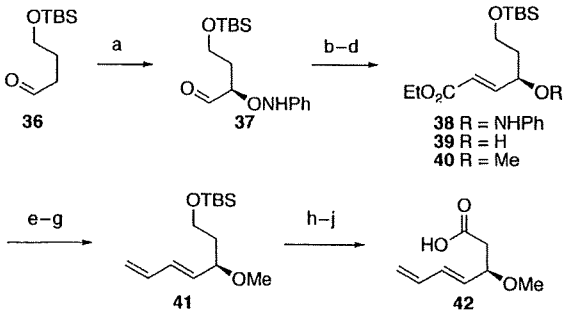

Scheme 2. Reagents and conditions: a) nitrosobenzene, L-proline, MeCN, −20°C, 24 h; b) triethyl phosphonoacetate, NaH, THF, 23°C, 45 min; c) $CuSO_4$, MeOH, 0°C, 46 h (46% from **36**, 98% *ee*); d) MeI, NaH, DMF, 0°C, 1 h (94%); e) DIBAL-H, CH_2Cl_2, −78°C to −40°C, 2 h; f) MnO_2, CH_2Cl_2, 23°C, 2 h; g) $[Ph_3P^+CH_3]I^-$, *t*BuOK, THF, 0°C, 15 min (66% from **40**); h) $py(HF)_x$, MeCN, 0°C, 1.5 h; i) SO_3·py, DMSO, Et_3N, CH_2Cl_2, 0°C, 50 min; j) $NaClO_2$, $NaH_2PO_4 \cdot 2H_2O$, 2-methyl-2-butene, *t*BuOH/H_2O (3:1), 23°C, 1 h (56% from **41**).

alcohol **39** by treatment with $CuSO_4$ in MeOH giving 46% yield (over 3 steps) with 98% *ee*. Williamson ether synthesis gave **40** in 94% yield. Diene **41** was synthesized by a three-step procedure: reduction with DIBAL-H, oxidation with MnO_2, and a Wittig reaction ($Ph_3P{=}CH_2$). Carboxylic acid **42** was constructed by removal of the TBS group, oxidation with SO_3·pyridine,[25] and subsequent oxidation by the method of Pinnick and co-workers.[26]

All that remained to complete the synthesis was the crucial ring formation. The protecting group of the phenol was converted from methyl to the more easily removable TES group through an oxidation/reduction sequence: 1) oxidation to the quinone with MnO_2, 2) reduction to hydroquinone **31** with $NaBH_4$, 3) immediate protection of **31** with 4-triethylsiloxy-3-penten-2-one[27] (this was the best silylating reagent in this particular case as low yields were obtained with other reagents because of the facile oxidation of hydroquinone **31** to quinone by adventitious O_2). Next RCM methodology, which had been used by Panek and co-workers in the synthesis of the core lactam of cytotrienin, was employed.[9] This reaction proceeded slowly when catalyzed by the first-generation Grubbs catalyst to afford triene in 39% yield along with recovered starting material **32** (23%), and therefore, a good conversion (51% brsm) was obtained. Removal of the TES group with Amberlyst 15 gave (+)-cytotrienin A (**1**) in 95% yield. Synthetic cytotrienin A exhibited spectroscopic properties identical to those of the natural product[1] (^{1}H NMR and IR spectroscopy, R_f value, optical rotation, and HPLC analysis) which confirms the absolute stereochemistry.

In summary, the first asymmetric total synthesis of (+)-cytotrienin A has been achieved, and its absolute configuration has been confirmed. There are several noteworthy features to this total synthesis: a practical diastereo- and

enantioselective aldol reaction using novel catalyst **33** under solvent-free conditions, highly diastereoselective construction of the three contiguous chiral centers, a deoxygenation reaction without positional or *E*/*Z* isomerization (from **10** to **11**), desulfonylation using $NaBH_4$ (from **21** to **22**), control of the absolute configuration at C3 by proline-mediated α-aminoxylation, and RCM for the formation of the 21-membered macrolactam.

Received: May 2, 2008
Published online: July 21, 2008

Keywords: aldol reaction · asymmetric synthesis · organocatalysis · ring-closing metathesis · total synthesis

[1] a) H. P. Zhang, H. Kakeya, H. Osada, *Tetrahedron Lett.* **1997**, *38*, 1789; b) H. Kakeya, H. P. Zhang, K. Kobinata, R. Onose, C. Onozawa, T. Kudo, H. Osada, *J. Antibiot.* **1997**, *50*, 370; c) H. Osada, H. Kakeya, H. P. Zhang, K. Kobinata, WO 9823594, **1998**; d) H. P. Zhang, H. Kayeka, H. Osada, *Tetrahedron Lett.* **1998**, *39*, 6947; e) H. Kakeya, R. Onose, H. Osada, *Cancer Res.* **1998**, *58*, 4888.

[2] a) M. Sugita, Y. Natori, T. Sasaki, K. Furihata, A. Shimazu, H. Seto, N. Otake, *J. Antibiot.* **1982**, *35*, 1460; b) M. Sugita, T. Sasaki, K. Furihata, A. Shimazu, H. Seto, N. Otake, *J. Antibiot.* **1982**, *35*, 1467; c) A. B. Smith III, J. L. Wood, W. Wong, A. E. Gould, C. J. Rizzo, J. Barbosa, K. Komiyama, S. Omura, *J. Am. Chem. Soc.* **1996**, *118*, 8308.

[3] a) S. Funayama, K. Okada, K. Komiyama, I. Umezawa, *J. Antibiot.* **1985**, *38*, 1107; b) S. Funayama, K. Okada, K. Iwasaki, K. Komiyama, I. Umezawa, *J. Antibiot.* **1985**, *38*, 1677; c) H. Nomoto, S. Katsumata, K. Takahashi, S. Funayama, K. Komiyama, I. Umezawa, S. Omura, *J. Antibiot.* **1989**, *42*, 479.

[4] a) N. Hosokawa, H. Naganawa, H. Inuma, M. Hamada, T. Takeuchi, T. Kanbe, M. Hori, *J. Antibiot.* **1995**, *48*, 471; b) A. B. Smith III, J. Barbosa, N. Hosokawa, H. Naganawa, T. Takeuchi, *Tetrahedron Lett.* **1998**, *39*, 2891.

[5] a) E. Tashiro, N. Hironiwa, M. Kitagawa, Y. Futamura, S. Suzuki, M. Nishio, M. Imoto, *J. Antibiot.* **2007**, *60*, 547; b) Y. Futamura, E. Tashiro, N. Hironiwa, J. Kohno, M. Nishio, K. Shindo, M. Imoto, *J. Antibiot.* **2007**, *60*, 582.

[6] A. B. Smith III, J. Barbosa, W. Wong, J. L. Wood, *J. Am. Chem. Soc.* **1996**, *118*, 8316.

[7] C. E. Masse, M. Yang, J. Solomon, J. S. Panek, *J. Am. Chem. Soc.* **1998**, *120*, 4123.

[8] A. B. Smith III, Z. Wan, *J. Org. Chem.* **2000**, *65*, 3738.

[9] G. Evano, J. V. Schaus, J. S. Panek, *Org. Lett.* **2004**, *6*, 525.

[10] D. Kashin, A. Meyer, R. Wittenberg, K.-U. Schoning, S. Kamlage, A. Kirschning, *Synthesis* **2007**, 304.

[11] Reviews; a) A. Fürstner, *Angew. Chem.* **2000**, *112*, 3140; *Angew. Chem. Int. Ed.* **2000**, *39*, 3012; b) T. M. Trnka, R. H. Grubbs, *Acc. Chem. Res.* **2001**, *34*, 18; c) R. H. Grubbs, *Tetrahedron* **2004**, *60*, 7117; d) K. C. Nicolaou, P. G. Bulger, D. Sarlah, *Angew. Chem.* **2005**, *117*, 4564; *Angew. Chem. Int. Ed.* **2005**, *44*, 4490.

[12] Review of total synthesis using organocatalysis; R. Marcia de Figueiredo, M. Christmann, *Eur. J. Org. Chem.* **2007**, 2575.

[13] A. B. Northrup, D. W. C. MacMillan, *J. Am. Chem. Soc.* **2002**, *124*, 6798.

[14] Y. Hayashi, S. Aratake, T. Okano, J. Takahashi, T. Sumiya, M. Shoji, *Angew. Chem.* **2006**, *118*, 5653; *Angew. Chem. Int. Ed.* **2006**, *45*, 5527.

[15] M. Suzuki, Y. Morita, H. Koyano, M. Koga, R. Noyori, *Tetrahedron* **1990**, *46*, 4809.

[16] The corresponding vinyl lithium gave a 1:1 mixture of diastereomers.

[17] C. S. Foote, M. T. Wuesthoff, S. Wexler, I. G. Burstain, R. Denny, G. O. Schenck, K.-H. Schulte-Elte, *Tetrahedron* **1967**, *23*, 2583.

[18] J.-L. Luche, *J. Am. Chem. Soc.* **1978**, *100*, 2226.

[19] a) J. Tsuji, I. Shimizu, I. Minami, *Chem. Lett.* **1984**, 1017; b) J. L. Hubbs, C. H. Heathcock, *J. Am. Chem. Soc.* **2003**, *125*, 12836.

[20] M. C. Pirrung, G. M. McGeehan, *J. Org. Chem.* **1983**, *48*, 5143.

[21] H. Bayley, D. N. Standring, J. R. Knowles, *Tetrahedron Lett.* **1978**, *19*, 3633.

[22] K. Nakamura, T. Nakajima, H. Kayahara, E. Nomura, H. Taniguchi, *Tetrahedron Lett.* **2004**, *45*, 495.

[23] J. M. Lalancette, A. Frche, J. R. Brindle, M. Laliberté, *Synthesis* **1972**, 526.

[24] a) Y. Hayashi, J. Yamaguchi, K. Hibino, M. Shoji, *Tetrahedron Lett.* **2003**, *44*, 8293; b) Y. Hayashi, J. Yamaguchi, T. Sumiya, M. Shoji, *Angew. Chem.* **2004**, *116*, 1132; *Angew. Chem. Int. Ed.* **2004**, *43*, 1112; c) Y. Hayashi, J. Yamaguchi, T. Sumiya, K. Hibino, M. Shoji, *J. Org. Chem.* **2004**, *69*, 5966; d) G. Zhong, *Angew. Chem.* **2003**, *115*, 4379; *Angew. Chem. Int. Ed.* **2003**, *42*, 4247; e) S. P. Brown, M. P. Brochu, C. J. Sinz, D. W. C. MacMillan, *J. Am. Chem. Soc.* **2003**, *125*, 10808; f) A. Bogevig, H. Sunden, A. Cordova, *Angew. Chem.* **2004**, *116*, 1129; *Angew. Chem. Int. Ed.* **2004**, *43*, 1109.

[25] J. R. Parikh, W. v. E. Doering, *J. Am. Chem. Soc.* **1967**, *89*, 5505;

[26] B. S. Bal, W. E. Childers Jr. , H. W. Pinnick, *Tetrahedron* **1981**, *37*, 2091.

[27] M. Egbertson, S. J. Danishefsky, G. Schulte, *J. Org. Chem.* **1987**, *52*, 4424.

[28] Alloc = allyloxycarbonyl, Boc = *tert*-butyloxycarbonyl, BOP-Cl = bis(2-oxo-3-oxazolidinyl)phosphinic chloride, DABCO = 1,4-diazabicyclo[2.2.2]octane, dba = *trans,trans*-dibenzylideneacetone, DDQ = 2,3-dichloro-5,6-dicyano-1,4-benzoquinone, DIBAL-H = diisobutylaluminum hydride, DMAP = 4-dimethylaminopyridine, DMF = *N,N*-dimethylformamide, DMSO = dimethyl sulfoxide, EDCI = 1-(3-dimethylaminopropyl)-3-ethylcarbodiimide hydrochloride, LHMDS = lithium hexamethyldisilazaide, PPTS = pyridinium *p*-toluenesulfonate, py = pyridine, TES = triethylsilyl, Tf = trifluoromethanesulfonyl, TIPS = triisopropylsilyl, Tr = trityl, Ts = 4-toluenesulfonyl.

Biosci. Biotechnol. Biochem., 72 (7), 1894–1900, 2008

Epoxyquinol B, a Naturally Occurring Pentaketide Dimer, Inhibits NF-κB Signaling by Crosslinking TAK1

Hiroshi KAMIYAMA,[1,2] Takeo USUI,[3] Hiroaki SAKURAI,[4] Mitsuru SHOJI,[5,*] Yujiro HAYASHI,[5] Hideaki KAKEYA,[1,**] and Hiroyuki OSADA[1,2,†]

[1]*Antibiotics Laboratory, RIKEN Advanced Science Institute, 2-1 Hirosawa, Wako, Saitama 351-0198, Japan*
[2]*Graduate School of Science and Engineering, Saitama University, 255 Shimo-okubo, Sakura-ku, Saitama 338-8570, Japan*
[3]*Graduate School of Life and Environmental Sciences, University of Tsukuba, 1-1-1 Tennodai, Tsukuba, Ibaraki 305-8572, Japan*
[4]*Division of Pathogenic Biochemistry, Institute of Natural Medicine, University of Toyama, 2630 Sugitani, Toyama 930-0194, Japan*
[5]*Department of Industrial Chemistry, Faculty of Engineering, Tokyo University of Science, 1-3 Kagurazaka, Shinjuku-ku, Tokyo 162-8601, Japan*

Received March 6, 2008; Accepted April 14, 2008; Online Publication, July 7, 2008
[doi:10.1271/bbb.80142]

Several epoxyquinoids interfere with NF-κB signaling by targeting IKKβ or NF-κB. We report that epoxyquinol B (EPQB), classified as an epoxyquiniod, inhibits NF-κB signaling through inhibition of the TAK1 complex, a factor upstream of IKKβ and NF-κB. cDNA microarray analysis revealed that EPQB decreased TNF-α-induced expression of NF-κB target genes. EPQB covalently bound to a recombinant TAK1-TAB1 fusion protein *in vitro*, and inhibited its kinase activity. Furthermore, *in vitro*/*in situ* treatment with EPQB resulted in a ladder-like hypershift of TAK1 protein bands. We reported recently that EPQB crosslinks proteins *via* cysteine residues by opening its two epoxides, and our current results suggest that EPQB inhibits NF-κB signaling by crosslinking TAK1 itself or TAK1 through other proteins.

Key words: epoxyquinol B; crosslink; TAK1; NF-κB

Epoxyquinoids exert anti-inflammatory effects by inhibiting nuclear factor κB (NF-κB) signaling.[1] Dehydroxymethylepoxyquinomicin (DHMEQ) delivers anti-inflammatory and antitumor effects by inhibiting the nuclear translocation of NF-κB.[2] Jesterone dimer, which is structurally similar to epoxyquinols, also inhibits NF-κB activation.[3] Moreover, several epoxyquinoids, for example, parthenolide, a sesquiterpen lactone isolated from the medicinal herb *Feverfew*,[4] manumycin A, an antibiotic from *Streptomyces parvulus*,[5] and epoxyquinone A monomer, a synthetic derivative of epoxyquinol,[6] have been reported to inhibit I-κB kinase (IKK) β kinase activity.

These inhibitory activities are thought to be mediated by the epoxide structure of epoxyquinoids, which reacts with nucleophiles, especially cysteine thiol groups. Parthenolide, manumycin A, and epoxyquinone A monomer bind directly to Cys-179 of IKK β, which is in the activation loop and plays a critical role in enzyme activation.[7]

We have found that epoxyquinol B (EPQB), a fungal metabolite and an epoxyquinoid that contains two epoxides, inhibits angiogenesis by covalently binding to cysteine residues of VEGFR2, EGFR, FGFR, and PDGFRβ.[8] Furthermore, we recently found that EPQB crosslinks proteins through cysteine residues by opening its two epoxides.[9] Hence, we hypothesized that EPQB inhibits signal transduction, including NF-κB signaling, through inter- and intramolecular crosslinking of target proteins.

Here, we report that EPQB blocks tumor necrosis factor-α (TNF-α)-induced NF-κB signaling through inhibition of TAK1, which plays a critical role in activating NF-κB signals. Additionally, EPQB binds directly to a TAK1-TAB1 fusion protein and crosslinks this protein complex. These findings suggest that EPQB inhibits NF-κB signaling by crosslinking pro-

† To whom correspondence should be addressed. Fax: +81-48-462-4669; E-mail: hisyo@riken.jp
* Present address: *Department of Chemistry, Graduate School of Science, Tohoku University, 6-3 Aramaki-Aza, Aoba, Sendai 980-8578, Japan*
** Present address: *Department of System Chemotherapy and Molecular Science, Division of Bioinformatics and Chemical Genomics, Graduate School of Pharmaceutical Sciences, Kyoto University, 46-29 Yoshida-Shimoadachi, Sakyo-ku, Kyoto 606-8501, Japan*

teins, including TAK1 itself or TAK1 through other proteins.

Materials and Methods

Cells and reagents. HeLa cells were cultured in Dulbecco's Modified Eagle's Medium (Sigma, St. Louis, MO) containing 10% heat-inactivated fetal calf serum (FCS) (JRH Bioscience, Lenexa, KS), 50 units/ml of penicillin, and 50 μg/ml of streptomycin (Sigma). Human umbilical vein endothelial cells (HUVECs) were cultured in HuMedia-EG2 (Kurabo, Osaka, Japan) containing 2% FCS in 5% CO_2 at 37 °C. Isolation and total synthesis of EPQB were performed as described previously.[10] Biotinylated EPQB (Bio-EPQB) was synthesized by oxime formation from EPQB and biotinylated alkoxyamine, which was prepared from 1,8-diamino-3,6-dioxaoctane *via* seven chemical transformations. The structure of biotinylated EPQB was determined by its physico-chemical properties, detailed ^{1}H- and ^{13}C-NMR analyses including two-dimensional techniques, and mass spectroscopies. Recombinant human TNF-α was purchased from Sigma.

Antibodies. Anti-phospho-TAK1 (Thr-187) antibody was described previously.[11,12] Anti-p65 rabbit polyclonal antibody (F-6), anti-IκB-α rabbit polyclonal antibody (C-21), anti-TAB1 goat polyclonal antibody (C-20), anti-TAB2 goat polyclonal antibody (E-20), anti-TAK1 rabbit polyclonal antibody (M-579), and anti-RIP rabbit polyclonal antibody (K-20) were purchased from Santa Cruz Biotechnology (Santa Cruz, CA). Anti-phospho-I-κB-α rabbit polyclonal antibody (#9241), anti-IKKβ rabbit polyclonal antibody (#2684), and anti-phospho-IKKβ rabbit polyclonal antibody (#2694), were from Cell Signaling Technology (Beverly, MA).

cDNA microarray analysis. HUVECs (2×10^6 cells/well) were cultured and treated with and without EPQB for 2 h. After stimulation with TNF-α (20 ng/ml) for 1 h, total RNA was extracted using ISOGEN (Nippon Gene, Tokyo). Next, cDNA microarray analysis was performed using the cDNA GEArray Human NF-κB Signaling Kit (SuperArray, Frederick, MD). The gene expression profiles determining upregulation or downregulation of genes after EPQB treatment were compared using GEArray analyzer software (Super Array).

Immunofluorescence analysis. To investigate the localization of NF-κB p65, HeLa cells were incubated on glass coverslips with or without EPQB for 2 h and stimulated with 20 ng/ml of TNF-α for 40 min. Immunofluorescence analysis of NF-κB p65 was performed as described previously.[2] To quantify fluorescence localization in the nucleus, the numbers of p65-positive nuclei were counted. The data are the representative averages of triplicate experiments.

Plasmids and transfections. A Flag-tagged TAK1-expressing plasmid was transiently transfected into HeLa cells using the Fugene 6 transfection reagent (Roche Diagnostics, Germany). After 24 h of incubation, the transfected cells were treated with and without EPQB for 2 h and stimulated by TNF-α (20 ng/ml) for 5 min. The samples were analyzed by Western blotting.

Immunoprecipitation and Western blot analysis. HeLa cells and HEK293T cells (2×10^5 cell/well) were treated with and without EPQB for 2 h and stimulated with TNF-α (20 ng/ml) for 5 min. Immunoprecipitation and Western blot analysis were performed as described previously.[11,12] Proteins were visualized using the SuperSignal West Pico Chemiluminescent Substrate (Pierce, Rockford, IL).

TAK1 kinase assay. Human recombinant TAK1-TAB1 fusion protein (Upstate Biotechnology, Charlottesville, VA) and MKK6 (Jena Bioscience, Jena, Germany) were used in the TAK1 kinase assay. TAK1 kinase activity was analyzed as described.[11,12] The percentage of inhibition was quantified with a bioimage analyzer (Fujix BAS2000).

In vitro *binding assay.* In the *in vitro* competitive binding assay, human recombinant TAK1-TAB1 fusion protein (100 ng/sample) was incubated with and without 0.1, 1, and 10 mM EPQB for 1 h at 37 °C in 50 mM Tris–HCl (pH 7.4). Next, each sample was treated with biotinylated EPQB (Bio-EPQB) 8) at 0.5 mM for 1 h at 37 °C. These samples were detected by Western blotting.

Results

EPQB downregulates expression of NF-κB target genes

Natural and synthetic epoxyquinoids have been reported to inhibit NF-κB signaling.[1] Hence, we investigated the effects of EPQB on NF-κB signaling by measuring changes in gene expression in TNF-α-stimulated HUVECs using a cDNA microarray. After TNF-α stimulation several genes were upregulated, such as inhibitor of NF-κB (I-κB), vascular cell adhesion molecule-1 (VCAM-1), and E-selectin, as listed in Table 1.

In contrast, 30 μM EPQB abolished the upregulation of several TNF-α-induced genes (Fig. 1B and Table 1). Correlating with parallel changes in mRNA levels, EPQB significantly suppressed cell adhesion by inhibiting the expression of cell adhesion molecules, such as ICAM1, VCAM1, and E-selectin, at the protein level in a dose-dependent manner (Supplemental Fig. 1; see *Biosci. Biotechnol. Biochem.* Web site). These results suggest that EPQB has an inhibitory effect against TNF-α-induced NF-κB signals.

Table 1. Down-Regulated Genes upon Treatment with EPQB

Gene symbol	Gene name	Ratio#	Ratio*
ICAM1	Intercellular adhesion molecule 1 (CD54), human rhinovirus receptor	1.29	0.53
ICAM2	Intercellular adhesion molecule 2	1.01	0.38
IFNA1	Interferon, alpha 1	0.67	0.58
IL1A	Interleukin 1, alpha	1.98	0.66
IL8	Interleukin 8	1.13	0.65
JUN	V-jun sarcoma virus 17 oncogene homolog (avian)	0.87	0.70
TAK1	Mitogen-activated protein kinase kinase kinase 7 (MAP3K7)	1.11	0.51
NF-κB1	Nuclear factor of kappa light polypeptide gene enhancer in B-cells 1 (p105)	1.23	0.46
NF-κB2	Nuclear factor of kappa light polypeptide gene enhancer in B-cells 2 (p49/p100)	1.41	0.52
I-κBa	Nuclear factor of kappa light polypeptide gene enhancer in B-cells inhibitor, alpha	1.39	0.65
CCL2	Chemokine (C-C motif) ligand 2	1.09	0.72
E-selectin	Selectin E (endothelial adhesion molecule 1)	1.12	0.55
TNFAIP3	Tumor necrosis factor, alpha-induced protein 3	1.10	0.45
VCAM1	Vascular cell adhesion molecule 1	2.01	0.41

Ratio#: [TNF-α stimulated control sample/TNF-α non-stimulated control sample]
Ratio*: [TNF-α stimulated EPQB treatment sample/TNF-α stimulated control sample]

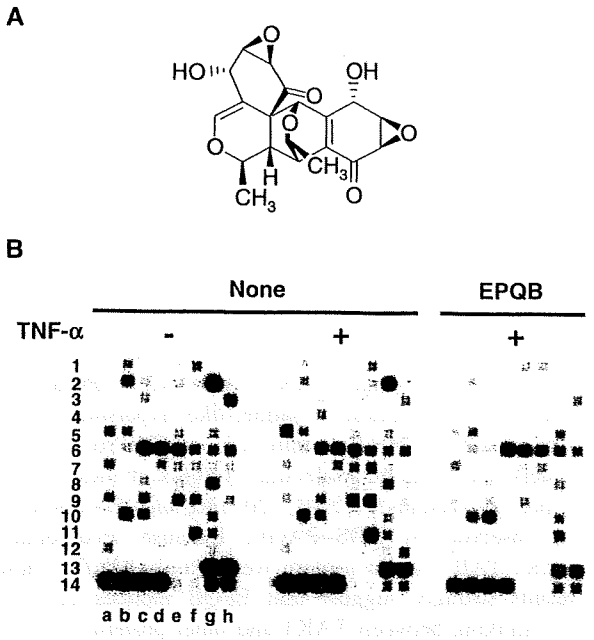

Fig. 1. Changes in TNF-α-Induced Gene Expression in HUVECs under EPQB Treatment.

A, Structure of epoxyquinol B (EPQB). B, cDNA microarray of NF-κB signaling. HUVECs were cultured and treated with and without EPQB for 2 h. After stimulation with and without TNF-α (20 ng/ml) for 1 h, total RNA was extracted. cDNA microarrays were assessed by cDNA GEArray for human NF-κB signaling. The up- and down-regulated genes were a-5, interleukin 8; c-3, interferon α1; c-4, interleukin 1 α; c-6, TAK1; d-7, NF-κB1; e-5, V-jun sarcoma virus 17 oncogene homolog; e-7, NF-κB2; e-9, Chemokine ligand 2; f-2, ICAM2; f-7, I-κBa; f-9, E-selectin; f-11, TNF-α induced protein 3; g-2, ICAM2; and h-12, VCAM1.

EPQB inhibits the nuclear translocation of NF-κB

Because nuclear translocation of NF-κB is vital to TNF-α-induced NF-κB signaling, we investigated the effect of EPQB on NF-κB p65 localization in HeLa cells. In most cells, NF-κB p65 was localized to the cytoplasm without TNF-α stimulation, and in only a fraction of the cells was p65 observed in the nuclei ($22.9 \pm 3.26\%$ cells). Forty minutes after TNF-α stimulation, NF-κB shuttled into the nuclei in most cells ($64.3 \pm 3.77\%$ cells), but this translocation was completely blocked by 10 μM EPQB ($28.1 \pm 2.32\%$ cells).

Moreover, an electrophoretic mobility shift assay using nuclear extract from EPQB-treated cells revealed that TNF-α-stimulated NF-κB binding to its target DNA was inhibited by EPQB in a dose-dependent manner. This inhibition did not occur, however, when EPQB was added to nuclear extract preparations of TNF-α treated cells (Supplemental Fig. 2; see *Biosci. Biotechnol. Biochem.* Web site). These results suggest that EPQB inhibits TNF-α-induced nuclear translocation of NF-κB.

EPQB inhibits TNF-α induced phosphorylation of TAK1 in situ *and the kinase activity of recombinant TAK1-TAB1 protein* in vitro

To characterize the effect of EPQB on TNF-α signaling, we examined TNF-α-induced phosphorylation of TAK1, IKKβ, and I-κB by Western blot. TAK1, IKKβ, and I-κB were dephosphorylated in unstimulated cells, but became significantly phosphorylated after TNF-α stimulation. Yet EPQB inhibited TNF-α-induced TAK1, IKKβ, and I-κB phosphorylation in a dose-dependent manner (Fig. 2A). Because TAK1 is upstream of IKKβ and I-κB, these results suggest that EPQB either inhibits TAK1 directly or acts on proteins that are upstream of TAK1.

TAK1 participates in the TAK1/TAB1/TAB2 complex, which is activated by polyubiquitin chain transfer from RIP to the zinc finger domain of TAB2.[13,14] Hence, we tested the effects of EPQB on TNF-α-induced RIP polyubiquitination by immunoprecipitation assay with anti-RIP antibody. As shown in Fig. 2B, RIP was polyubiquitinated after TNF-α stimulation, and EPQB did not inhibit the polyubiquitination of RIP.

Next we tested *in vitro* TAK1 kinase activity to determine whether EPQB would directly inhibit TAK1. Recombinant TAK1-TAB1 fusion protein phosphor-

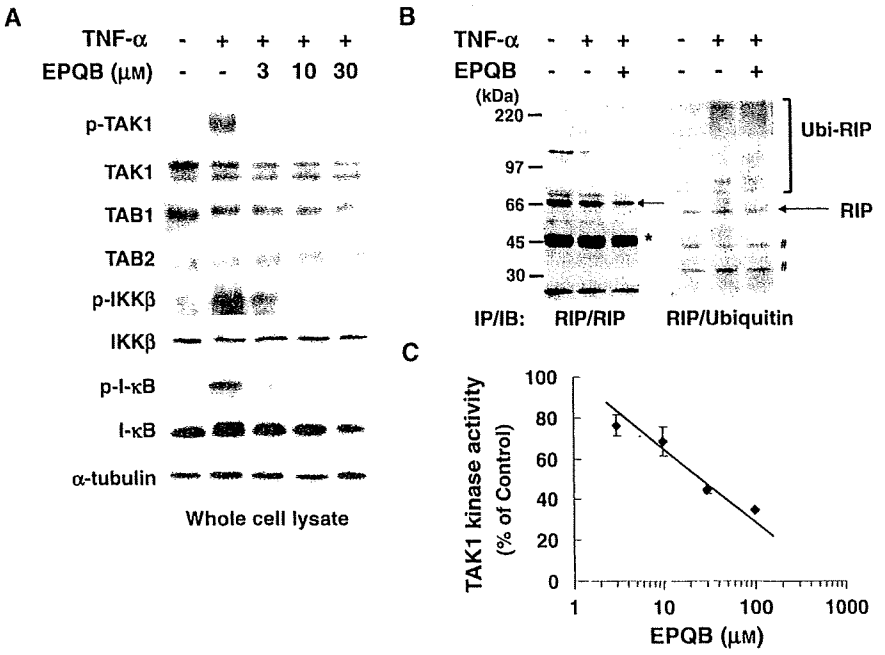

Fig. 2. Inhibition of TAK1 Activation in HeLa Cells.

A, Western blot analysis of phosphorylation of NF-κB signaling proteins. HeLa cells were treated with and without EPQB for 2 h and stimulated with 20 ng/ml of TNF-α for 5 min. p-TAK1, p-IKKβ, and p-I-κB indicate phosphorylated molecules. B, Polyubiquitination of RIP. HEK293T cells were stimulated with or without TNF-α for 5 min. Samples were immunoprecipitated with anti-RIP antibody and analyzed by Western blot. The asterisk denotes the heavy chain band, and # indicates a nonspecific band. C, *In vitro* TAK1 kinase assay. Human recombinant TAK1-TAB1 protein was incubated with and without EPQB, and was subjected to kinase reactions with MKK6 and γ-[^{32}P] ATP. The percentage of kinase inhibition was quantified with a bioimage analyzer.

ylated MKK6, but EPQB inhibited TAK1 kinase activity in a dose-dependent manner (Fig. 2C). These results suggest that EPQB directly inhibits TAK1 activity in NF-κB signaling.

EPQB covalently binds TAK1-TAB1 fusion protein

Because EPQB directly inhibits TAK1 kinase activity, we anticipated that EPQB would bind to TAK1. To investigate this possibility, we tested the binding of EPQB to a recombinant TAK1-TAB1 fusion protein using Bio-EPQB. As shown in Fig. 3A, Bio-EPQB covalently bound to the TAK1-TAB1 fusion protein, and its binding was precluded by EPQB in a dose-dependent manner. The binding between TAK1-TAB2 fusion protein and Bio-EPQB was inhibited by cysteine and glutathione, but not by serine (Supplemental Fig. 3; see *Biosci. Biotechnol. Biochem.* Web site). These results suggest that EPQB covalently binds to TAK1-TAB1/2 complex through cysteine residues.

EPQB crosslinks TAK1 and inhibits NF-κB signaling

When EPQB was administered to Flag-tagged TAK1-overexpressed cells, we noticed that several hypershifted bands appeared in an EPQB-dependent manner (Fig. 3B the left panel). Because these proteins did not represent polyubiquitinated bands (Supplemental Fig. 4; see *Biosci. Biotechnol. Biochem.* Web site), this result suggests that Flag-tagged TAK1 was covalently incorporated into high-molecular weight complexes. Furthermore, treatment of recombinant TAK1-TAB1 with EPQB also elicited the formation of ladder-like hypershifted variants of TAK1-TAB1 protein *in vitro* (Fig. 3B the right panel); the apparent molecular weights of these newly appearing proteins were 90, 120–140, and 170–200 kDa, as observed by SDS–PAGE. Because recombinant TAK1-TAB1 fusion protein weighs only 45 kDa, these results strongly suggest that EPQB induces covalent crosslinking between TAK1 and other proteins.

To exclude the possibility that NF-κB signaling is inhibited only by cysteine modification and not by crosslinking, we treated cells with *N*-ethylmaleimide (NEM), a nonspecific and cell-permeable thiol binder. NEM did not inhibit TAK1 phosphorylation, suggesting that cysteine residues are not involved in TAK1 activation (Supplemental Fig. 5; see *Biosci. Biotechnol. Biochem.* Web site).

Before stimulation with EPQB and TNF-α, Flag-tagged TAK1-overexpressed cells were treated with and without NEM to block the cysteine residues that bind to EPQB. Then TAK1 proteins were immunoprecipitated and analyzed by Western blot. As shown in Fig. 3C, TAK1 crosslinking was inhibited by NEM pretreatment, suggesting that NEM modified the cysteine residues targeted by EPQB. Under this condition, EPQB failed to inhibit the phosphorylation of TAK1, suggesting that modification of the cysteine residues alone is insufficient

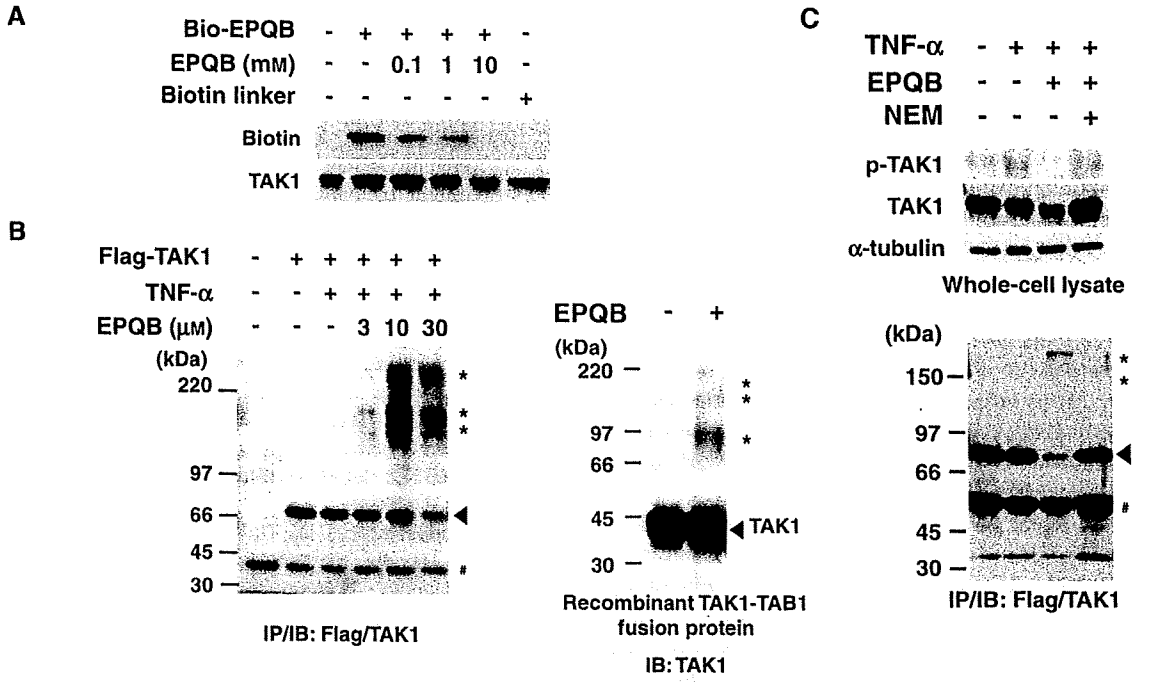

Fig. 3. EPQB Covalently Binds and Crosslinks TAK1 Proteins.

A, Binding assay between EPQB and TAK1. Recombinant TAK1-TAB1 fusion protein was pretreated with and without EPQB at various concentrations for 1 h as the competitor, and then incubated with Bio-EPQB at 0.5 mM for 1 h at 37 °C. The samples were analyzed by Western blot. B, Appearance of supershifted bands containing TAK1 under EPQB treatment. Flag-TAK1-overexpressing HeLa cells were treated with EPQB at various concentrations for 2 h. The samples were immunoprecipitated with anti-Flag antibody (left panel). Recombinant TAK1-TAB1 fusion protein (45 kDa) was treated with EPQB at 10 mM for 2 h *in vitro* (right panel). These samples were analyzed by Western blot. C, Flag-TAK1-overexpressing HeLa cells were pretreated with *N*-ethylmaleimide for 1 h at 300 μM and treated with EPQB at 30 μM for 1 h. These samples were immunoprecipitated with anti-Flag antibody and analyzed by Western blot. The asterisk denotes a supershifted band, and # indicates a nonspecific band. The arrow head indicates TAK1 protein band (77 kDa).

for TAK1 inhibition. Instead, crosslinking of EPQB to TAK1 or to TAK1 and other proteins appears to be critical to EPQB-mediated inhibition.

Discussion

NF-κB activation occurs in rheumatoid arthritis, kidney inflammation, and malignant tumor growth.[15–17] Hence, pharmaceutical inhibitors of NF-κB activation have been screened and developed as potential therapeutic agents. Because Cys179 of IKKβ has been reported to be the target of several fungus-derived epoxyquinoids,[4–6] we examined the effects of EPQB on NF-κB signaling by cDNA microarray.

We found that EPQB inhibited the expression of TNF-α-induced genes, such as NF-κB, I-κB, ICAM1, VCAM1, and E-selectin (Fig. 1B). In addition, it significantly inhibited nuclear translocation of NF-κB and TAK1 phosphorylation at Thr187 (Fig. 2A). Because phosphorylation of TAK1 at Thr187 is crucial to IKK activation and subsequently to NF-κB,[12] we focused on the inhibition of TAK1 activation by EPQB.

TAK1 is one of the most well-characterized mitogen-activated protein kinase kinase kinases, and the binding of polyubiquitinated RIP *via* the TAB2 zinc finger domain is necessary to TAK1 activation.[18,19] Hence we examined to determine whether TAK1 kinase activity and RIP polyubiquitination would be inhibited by EPQB.

Immunoprecipitation analysis revealed that EPQB did not inhibit RIP polyubiquitination (Fig. 2B). Furthermore, EPQB inhibited the kinase activity of the TAK1-TAB1 fusion protein in a dose-dependent manner (Fig. 2C). These results strongly suggest that EPQB inhibits TAK1 activity directly in the context of TNF-α-induced NF-κB signaling.

Although TAK1 plays a critical role in the activation of NF-κB signaling, few inhibitors of TAK1 have been reported. 5Z-7-oxozeaenol, a resorcylic lactone of fungal origin, inhibits the interleukin-induced activation of TAK1, IKK, JNK, p38, and NF-κB *in vitro* and shows anti-inflammatory activity *in vivo*.[20] This report also suggests that a TAK1 inhibitor is a potential candidate for the inhibitor of NF-κB signaling.

In this study, we found that EPQB covalently bound recombinant TAK1-TAB1 fusion protein (Fig. 3A) and, that EPQB induced crosslinking to TAK1 itself, or to TAK1 and other proteins, which might cause inhibition of NF-κB signaling (Fig. 3B, C). We reported recently that EPQB showed anti-angiogenic effects, and covalently bound to two cysteines.[8] Furthermore, we found that EPQB crosslinked through cysteine residues on

recombinant VEGFR2 kinase protein in an EPQB-dependent manner.[9] These results suggest that EPQB has multiple targets, and that the crosslinking of target proteins induces inhibition of several signal transductions. There are a few reports that compounds crosslink two cysteines of target proteins. Guido *et al.* has suggested that helenalin, a sesquiterpene lactone, crosslinks proteins through cysteine residues on NF-κB.[21] Because the active site of NF-κB contains several cysteine residues, helenalin might affect NF-κB signaling by binding and crosslinking to it. The kinase activation loop of TAK1, which contains an autophosphorylation site at threonine residues (Thr184 and Thr187) and a serine residue (Ser192), also contains a cysteine residue (Cys180).[22] Therefore, we propose that EPQB inhibits NF-κB signaling through EPQB-induced crosslinking with TAK1 and other proteins.

In this study, we found that EPQB inhibits TNF-α-induced TAK1 activity by crosslinking to TAK1 itself or to TAK1 and other proteins. These results strongly suggest that the mechanism of inhibition of EPQB differs from that of other epoxyquinoids, because EPQB harbors a highly reactive element that contains two epoxides. Hence, EPQB might be a good lead compound to design a crosslinking agent to prevent signal transduction.

Acknowledgment

This study was supported in part by Junior Research Associate Program, by the Grants for Basic Research (Chemical Biology Project) from RIKEN, and a Grant-in-Aid from the Ministry of Education, Culture, Sports, Science, and Technology of Japan. We thank Naoki Kanoh of Tohoku University for technical advice and useful discussion.

References

1) Bremner, P., and Heinrich, M., Natural products as targeted modulators of the nuclear factor-κB pathway. *J. Pharm. Pharmacol.*, **54**, 453–472 (2002).
2) Ariga, A., Namekawa, J., Matsumoto, N., Inoue, J., and Umezawa, K., Inhibition of tumor necrosis factor-α-induced nuclear translocation and activation of NF-κB by dehydroxymethylepoxyquinomicin. *J. Biol. Chem.*, **277**, 24625–24630 (2002).
3) Liang, M., Bardhan, S., Li, C., Pace, E. A., Porco, J. A., Jr., and Gilmore, T. D., Jesterone dimer, a synthetic derivative of the fungal metabolite jesterone, blocks activation of transcription factor nuclear factor κB by inhibiting the inhibitor of κB kinase. *Mol. Pharmacol.*, **64**, 123–131 (2003).
4) Kwok, B. H., Koh, B., Ndubuisi, M. I., Elofsson, M., and Crews, C. M., The anti-inflammatory natural product parthenolide from the medical herb *feverfew* directly binds to and inhibits IκB kinase. *Chem. Biol.*, **8**, 759–766 (2001).
5) Bernier, M., Kwon, Y. K., Pandey, S. K., Zhu, T. N., Zhao, R. J., Maciuk, A., He, H. J., DeCabo, R., and Kole, S., Binding of manumycin A inhibits IκB kinase β activity. *J. Biol. Chem.*, **281**, 2551–2561 (2006).
6) Liang, M., Bardhan, S., Pace, E. M., Rosman, D., Beutler, J. A., Porco, J. A., Jr., and Gilmore, T. D., Inhibition of transcription factor NF-κB signaling proteins IKKβ and p65 through specific cysteine residues by epoxyquinone A monomer: correlation with its anti-cancer cell growth activity. *Biochem. Pharmacol.*, **71**, 634–645 (2006).
7) Byun, M. S., Choi, J., and Jue, D. M., Cysteine-179 of IkappaB kinase beta plays a critical role in enzyme activation by promoting phosphorylation of activation loop serines. *Exp. Mol. Med.*, **38**, 546–552 (2006).
8) Kamiyama, H., Kakeya, H., Usui, T., Nishikawa, K., Shoji, M., Hayashi, Y., and Osada, H., Epoxyquinol B shows antiangiogenic and antitumor effects by inhibiting VEGFR2, EGFR, FGFR, and PDGFR. *Oncol. Res.*, **17**, 11–21 (2008).
9) Kamiyama, H., Usui, T., Uramoto, M., Takagi, H., Shoji, M., Hayashi, Y., Kakeya, H., and Osada, H., A fungal metabolite, Epoxyquinol B, crosslinks proteins by epoxy-thiol conjugation. *J. Antibiotics*, **61**, 94–97 (2008).
10) Shoji, M., Yamaguchi, J., Kakeya, H., Osada, H., and Hayashi, Y., Total synthesis of (+)-epoxyquinols A and B. *Angew. Chem. Int. Ed. Engl.*, **41**, 3192–3194 (2002).
11) Sakurai, H., Miyoshi, H., Toriumi, W., and Sugita, T., Functional interactions of transforming growth factor beta-activated kinase 1 with IkappaB kinases to stimulate NF-κB activation. *J. Biol. Chem.*, **274**, 10641–10648 (1999).
12) Singhirunnusorn, P., Suzuki, S., Kawasaki, N., Saiki, I., and Sakurai, H., Critical roles of threonine 187 phosphorylation in cellular stress induced rapid and transient activation of transforming growth factor-β-activated kinase 1 (TAK1) in a signaling complex containing TAK1-binding protein TAB1 and TAB2. *J. Biol. Chem.*, **280**, 7359–7368 (2005).
13) Chen, Z. J., Ubiquitin signaling in the NF-κB pathway. *Nat. Cell Biol.*, **8**, 758–765 (2005).
14) Kanayama, A., Seth, R. B., Sun, L., Ea, C. K., Hong, M., Shaito, A., Chiu, Y. H., Deng, L., and Chen, Z. J., TAB2 and TAB3 activate the NF-κ B pathway through binding to polyubiquitin chains. *Mol. Cell*, **15**, 535–548 (2004).
15) Hoffmann, J. A., Kafatos, F. C., Janeway, C. A., and Ezekowitz, R. A. B., Phylogenetic perspectives in innate immunity. *Science*, **284**, 1313–1318 (1999).
16) Ghosh, S., May, M. J., and Kopp, E. B., NF-κB and REL proteins: evolutionary conserved mediators of immune responses. *Annu. Rev. Immunol.*, **16**, 225–260 (1998).
17) Calzado, M. A., Bacher, S., and Schmitz, M. L., NF-κB inhibitors for the treatment of inflammatory diseases and cancer. *Curr. Med. Chem.*, **14**, 367–376 (2007).
18) Shirakabe, K., Yamaguchi, K., Shibuya, H., Irie, K., Matsuda, S., Moriguchi, T., Gotoh, Y., Matsumoto, K., and Nishida, E., TAK1 mediates the ceramide signaling to stress-activated protein kinase/c-Jun N-terminal kinase. *J. Biol. Chem.*, **272**, 8141–8144 (1997).
19) Ninomiya-Tsuji, J., Kishimoto, K., Hiyama, A., Inoue, J., Cao, Z., and Matsumoto, K., The kinase TAK1 can activate the NIK-I κ B as well as the MAP kinase cascade in the IL-1 signaling pathway. *Nature*, **398**,

252–256 (1999).
20) Ninomiya-Tsuji, J., Kajino, T., Ono, K., Ohtomo, T., Matsumoto, M., Shiina, M., Mihara, M., Tsuchiya, M., and Matsumoto, K., A resorcylic acid lactone, 5Z-7-oxozeaenol, prevents inflammation by inhibiting the catalytic activity of TAK1 MAPK kinase. *J. Biol. Chem.*, **278**, 18485–18490 (2003).
21) Guido, L., Knorre, A., Schmidt, T. J., Pahl, H. L., and Merfort, I., The anti-inflammatory sesquiterpene lactone helenalin inhibits the transcription factor NF-κB by directly targeting p65. *J. Biol. Chem.*, **273**, 33508–33516 (1998).
22) Brown, K. B., Vial, S. C., Dedi, N., Long, J. M., Dunster, N. J., and Cheetham, G. M. T., Structural basis for the interaction of TAK1 kinase with its activating protein TAB1. *J. Mol. Biol.*, **354**, 1013–1020 (2005).

(Selected as an issue highlight and a cover page.)

Azaspirene, a fungal product, inhibits angiogenesis by blocking Raf-1 activation

Yukihiro Asami,[1,5] Hideaki Kakeya,[1,6] Yusuke Komi,[2] Soichi Kojima,[2] Kiyohiro Nishikawa,[3] Kristin Beebe,[4] Len Neckers[4] and Hiroyuki Osada[1,7]

[1]Antibiotics Laboratory, Advanced Science Institute, RIKEN, 2-1 Hirosawa, Wako, Saitama 351-0198; [2]Molecular Cellular Pathology Research Unit, RIKEN, 2-1 Hirosawa, Wako, Saitama 351-0198; [3]R. and D. Division, Pharmaceuticals Group, Nippon Kayaku, 31-12 Shimo 3-chome, Kita-ku, Tokyo 115-8588, Japan; [4]Urologic Oncology Branch, National Cancer Institute, 9000 Rockville Pike, Building 10/CRC, 1-5940, Bethesda, Maryland 20892, USA

(Received January 18, 2008/Revised May 15, 2008/Accepted May 21, 2008/Online publication July 10, 2008)

Angiogenesis is an inevitable event in tumor progression and metastasis, and thus has been a compelling target for cancer therapy in recent years. Effective inhibition of tumor progression and metastasis could become a promising way to treat tumor-induced angiogenesis. We discovered that a fungus, *Neosartorya* sp., isolated from a soil sample, produced a new angiogenesis inhibitor, which we designated azaspirene. Azaspirene was previously shown to inhibit human umbilical vein endothelial cell (HUVEC) migration induced by vascular endothelial growth factor (VEGF) at an effective dose, 100% of 27 μmol/L without significant cell toxicity. In the present study, we investigated the antiangiogenic activity of azaspirene *in vivo*. Azaspirene treatment reduced the number of tumor-induced blood vessels. Administration of azaspirene at 30 μg/egg resulted in inhibition of angiogenesis (23.6–45.3% maximum inhibition relative to the controls) in a chicken chorioallantoic membrane assay. Next, we elucidated the molecular mechanism of antiangiogenesis of azaspirene. We investigated the effects of azaspirene on VEGF-induced activation of the mitogen-activated protein kinase signaling pathway in HUVEC. *In vitro* experiments indicated that azaspirene suppressed Raf-1 activation induced by VEGF without affecting the activation of kinase insert domain-containing receptor/fetal liver kinase 1 (VEGF receptor 2). Additionally, azaspirene preferentially inhibited the growth of HUVEC but not that of the non-vascular endothelial cells NIH3T3, HeLa, MSS31, and MCF-7. Taken together, these results demonstrate that azaspirene is a novel inhibitor of angiogenesis and Raf-1 activation that contains a unique carbon skeleton in its molecular structure. (*Cancer Sci* 2008; 99: 1853–1858)

The angiogenic process is tightly controlled by a wide variety of positive and negative regulators, including growth factors, cytokines, lipid metabolites, and cryptic fragments of hemostatic proteins.[1] Among these molecules, vascular endothelial growth factor (VEGF), a soluble angiogenic factor produced by many tumor and normal cells, plays a key role in regulating normal and abnormal angiogenesis.[2] Angiogenesis is also initiated in response to certain pathological conditions, such as solid tumor growth, diabetic retinopathy, psoriasis, and rheumatoid arthritis, in all of which angiogenesis is responsible for the disease progression.[3]

In particular, it is well-known that the growth of tumors larger than a few cubic millimeters requires continuous recruitment of new blood vessels.[4] Complex and diverse cellular actions are implicated in angiogenesis, namely extracellular matrix degradation, proliferation and migration of endothelial cells, and morphological differentiation of endothelial cells to form tubes.[3] These newly synthesized blood vessels also provide a route for cancer cells to enter the blood circulation and spread to other organs.[5] Therefore, the inhibition of angiogenesis is a promising strategy to treat tumors. In particular, research on VEGF receptors (VEGFR) has been a focus of angiogenesis research. VEGFR1 is required for the recruitment of hematopoietic precursors and for migration of monocytes and macrophages,[6] whereas VEGFR2 and VEGFR3 are essential for vascular endothelial and lymphendothelial cells, respectively.[7,8] Notably, the VEGFR2 signaling pathway is a promising target for inhibiting angiogenesis because it is a common pathway for tumor-induced angiogenesis.[9,10]

Especially, Raf-1 or Raf-1-interacting molecules are possible targets for antiangiogenic compounds.[11,12] In fact, various synthetic compounds that inhibit the VEGF, platelet-derived growth factor (PDGF), and epidermal growth factor (EGF) signaling pathways are under development, such as, vatalanib (PTK787/ZK222584), sorafenib (BAY 43-9006), and vandetanib (ZD6474/Zactima).[13–17] However, there have been relatively few reports of natural compounds with antiangiogenic activities.[18]

Hence, it is still important to explore new angiogenesis inhibitors from natural compounds. We have discovered several naturally occurring angiogenesis inhibitors, such as RK-805,[19] epoxyquinol A and B,[20,21] epoxytwinol A,[22] RK-95113,[23] and azaspirene, which has a 1-oxa-7-azaspiro[4.4]non-2-ene-4,6-dione skeleton and is derived from fungal metabolites.[24] In the present study, we report the antiangiogenic activity of azaspirene *in vivo* and reveal the molecular basis underlying it.

Materials and Methods

Reagents and antibodies. Azaspirene was prepared as described previously.[24] The selective kinase insert domain-containing receptor/fetal liver kinase 1 (KDR/Flk-1) tyrosine kinase inhibitor SU5614, MEK1 kinase inhibitor PD98059, and Hsp90 inhibitor geldanamycin were purchased from Calbiochem (La Jolla, CA, USA). Paclitaxel was purchased from Xi'an High-Tech Industries (Xian, China). Recombinant human VEGF was purchased from R & D Systems (Minneapolis, MN, USA). Recombinant human EGF, basic fibroblast growth factor (bFGF), and PDGF were purchased from Sigma-Aldrich (St Louis, MO, USA). Mouse monoclonal antibodies against phospho-tyrosine, MEK1, and MEK2 were purchased from Transduction Laboratories (Lexington, KY, USA), whereas antibodies against HSP90, Raf-1, phospho-Raf-1, phospho-ERK1/2, and phospho-MEK1/2 were purchased from Stressgen Biotechnologies (Victoria, BC, Canada), Santa Cruz Biotechnology (Santa Cruz, CA, USA), Upstate Biotechnology (Lake Placid, NY, USA), Cell Signaling Technology (Beverly, MA, USA), and Cell Signalling Technology, respectively. Rabbit

[5]Present address: Laboratory of Microbiology, Graduate School of Pharmaceutical Sciences, The University of Tokyo, 3-1, 7-chome, Hongo, Bunkyo-ku, Tokyo 113-0033, Japan.
[6]Present address: Department of System Chemotherapy and Molecular Sciences, Division of Bioinformatics and Chemical Genomics, Graduate School of Pharmaceutical Sciences, Kyoto University, 46-29 Yoshida-Shimoadachi, Sakyo-ku, Kyoto 606-8501, Japan.
[7]To whom correspondence should be addressed. E-mail: hisyo@riken.jp

doi: 10.1111/j.1349-7006.2008.00890.x

polyclonal antibodies against KDR/Flk-1, Raf-1, ERK1/2, and MEK1/2 were purchased from Santa Cruz Biotechnology, Zymed Laboratories (South San Francisco, CA, USA), Cell Signaling Technology, respectively. Blocking buffer and working concentrations of the above antibodies were prepared according to the manufacturers' instructions.

***In vivo* tumor-induced angiogenesis in a renal carcinoma xenograft model.** The assay for tumor-induced angiogenesis was carried out as described by Kreisle and Ershler.[25] Female BALB/c mice (7 weeks old; Charles River Laboratories, Tokyo, Japan) were used for *in vivo* experiments. BALB/c mice were injected intradermally (i.d.) with 1×10^6 murine renal carcinoma (RENCA) cells in the back on day 0. Mice were administered vehicle or paclitaxel (6 or 20 mg/kg, intraperitoneally [i.p.], daily) consisting of 5% ethanol and 5% polyoxyethylene castor oil in saline for days 0–6. Azaspirene was dissolved in normal saline containing 10% dimethyl sulfoxide (DSMO). Azaspirene (31.6 or 100 mg/kg, i.p.) was administered every second day (days 0, 2, 4, and 6). The animals were euthanized on day 7, and skin with tumors was separated from the underlying tissue. Tumor angiogenesis was quantified by counting the number of blood vessels oriented toward the tumor using a digital camera. The same observer made all counts. The present study was in accordance with the Helsinki Declaration of the World Medical Association and the guidelines of the ethical committees of the authors' institutions.

Chicken chorioallantoic membrane assay. The formation of new blood vessels within chicken chorioallantoic membrane (CAM) was assessed as described previously.[26] In brief, fertilized Dekalb chicken eggs (Omiya Kakin, Saitama, Japan) were placed in a humidified egg incubator. After a 4.5-day incubation at 38°C, a 1% solution of methylcellulose containing 30 μg azaspirene/egg was loaded inside a silicon ring placed on the surface of the CAM. After further incubation for 2 days, a fat emulsion was injected into the chorioallantois, such that the vascular networks stood out against the white background of the lipid. Antiangiogenic responses were evaluated under a stereomicroscope and photographed with a ×7.25 objective. Quantitative analyses were carried out with angiogenesis-measuring software (Kurabo Angiogenesis Image Analyzer, version 1.0; Kurabo, Osaka, Japan). Five eggs were analyzed in each treatment group, and all experiments were repeated three times.

Cell culture. MCF-7 cells were cultured in RPMI-1640 medium supplemented with 5% calf serum in the presence of 30 μg/mL penicillin and 42 μg/mL streptomycin under a humidified atmosphere of 5% CO_2 at 37°C. NIH3T3, HeLa, MSS31 (a mouse spleen stromal cell line; a gift from Dr. N. Yanai, Tohoku University), and HEK293T cells were cultured in Dulbecco's Modified Eagle's Medium containing 10% fetal calf serum (FCS) in 5% CO_2 at 37°C. Human umbilical vein endothelial cells (HUVEC) were cultured in Humedia-EG2 (Kurabo) at 37°C under a 5% CO_2 atmosphere. All cell experiments were carried out using HUVEC between passages three and six.

Western blotting. Pre-confluent NIH3T3, HeLa, MSS31, and MCF-7 cells were pretreated with serum-free medium. HUVEC were pretreated with M199 containing 2% FCS overnight and were left untreated or exposed to various concentrations of azaspirene for 60 min prior to the addition of various stimulators: VEGF (12.5 ng/mL), EGF (10 ng/mL), bFGF (10 or 25 ng/mL), PDGF (30 ng/mL), or phorbol 12, 13-dibutyrate (PDBu) (10 ng/mL). Twenty-five μmol/L PD98059 and 10 μmol/L SU5614 were used as a positive control for the MEK1 kinase inhibitor and the KDR/Flk-1 tyrosine kinase inhibitor, respectively. Western blotting experiments were prepared as described previously.[27,28]

Immunoprecipitation. Confluent HUVEC were pretreated with M199 containing 2% FCS medium overnight and were left untreated or exposed to various concentrations of azaspirene for 60 min prior to the addition of VEGF (12.5 ng/mL). SU5614 (10 μmol/L) and geldanamycin (10 μmol/L) were used as positive controls for KDR/Flk-1 tyrosine kinase inhibitor and Hsp90 inhibitor, respectively. The immunoprecipitation experiments were carried out as described previously.[29,30]

Cell proliferation assay. NIH3T3, HeLa, MSS31, MCF-7 and HUVEC were seeded on 96-well microplates (3.0×10^3 cells per well). Test compounds were dissolved in DMSO at appropriate concentrations and were treated for 48 h. Cell proliferation assays were carried out using the WST-8 (Nacalai Tesque, Kyoto, Japan) protocol. The absorbance (A_{450}) of each well was measured using a Wallac 1420 multilabel counter (Amersham Bioscience, Piscataway, NJ, USA).

Cell transfection. The expression plasmids bearing cDNA of KDR/Flk-1 were prepared as described previously.[31] We cloned the complementary DNA of KDR/Flk-1 into the *KpnI–XhoI* sites of the pcDNA4/TO vector (Invitrogen, Carlsbad, CA, USA). Transfection of pcDNA4/TO-KDR/Flk-1 plasmids was carried out using Fugene HD (Roche Diagnostics, Mannheim, Germany) according to the manufacturer's standard protocol.

Results

Azaspirene inhibited tumor-induced angiogenesis in a renal carcinoma xenograft model. As azaspirene (Fig. 1a) was isolated from fungal metabolites by screening with an endothelial cell migration assay, the inhibitory activity of azaspirene against tumor-induced angiogenesis was examined using murine RENCA cells *in vivo*. BALB/c mice received either azaspirene (31.6 or 100 mg/kg, i.p., every second day) or paclitaxel (6 or 20 mg/kg, i.p., daily) after inoculation of RENCA cells (1×10^6 cells/site) subcutaneously. The number of vessels oriented toward the tumor, the tumor volume, and the bodyweight were assessed after 7 days. As shown in Fig. 1b,c, the number of blood vessels oriented toward the tumor decreased with azaspirene treatment. The maximum dose of 100 mg/kg also showed a tendency to reduce the tumor volume. Although the reduction in tumor volume did not reach statistical significance, in contrast to paclitaxel, the antiangiogenic activity of azaspirene was not associated with a loss of bodyweight (data not shown). These results clearly indicate that azaspirene had antiangiogenic effects *in vivo*.

Azaspirene showed antiangiogenic activity in a chicken CAM assay. The antiangiogenic activity of azaspirene was investigated *in vivo* using a chicken CAM assay. After 2 days of incubation, azaspirene elicited an antiangiogenic response, which was visible under a microscope as a spoke-wheel-like pattern of blood vessels. Azaspirene produced a decrease in the development of angiogenesis in the chick embryo without any sign of thrombosis or hemorrhage (Fig. 2a). In Fig. 2b, azaspirene suppressed the neovascularization of chick embryo when compared to vehicle ($71.4 \pm 18.1\%$ of the value obtained with 10% DMSO, $n = 5$ in each group).

Azaspirene inhibited angiogenic factor-induced activation of MAPK in HUVEC. VEGF induces proliferation and migration through activation of its cell surface receptor, KDR/Flk-1.[32] To understand the molecular mechanism by which azaspirene exerts its antiangiogenic activities, we investigated the effects of azaspirene on VEGF-induced activation of MEK1/2 and ERK1/2, which are downstream signaling molecules of KDR/Flk-1. VEGF-induced MEK1/2 and ERK1/2 activations were significantly inhibited by azaspirene in a dose-dependent manner (Fig. 3a), and azaspirene suppressed the kinase cascade Raf-1–MEK–ERK pathway activated by three other stimulation factors, EGF, bFGF, and PDBu (Fig. 3b–d). These data suggest that azaspirene blocks upstream activation of the MAP kinase signaling pathway in HUVEC.

Azaspirene inhibited VEGF-induced Raf-1 activation without affecting tyrosine phosphorylation of KDR/Flk-1 or protein complexes of Raf-1. To examine the effect of azaspirene on the cellular mechanism of Raf-1 activation, formation of Raf-1 complexes, and phosphorylation of KDR/Flk-1 in HUVEC, we studied the

doi: 10.1111/j.1349-7006.2008.00890.x

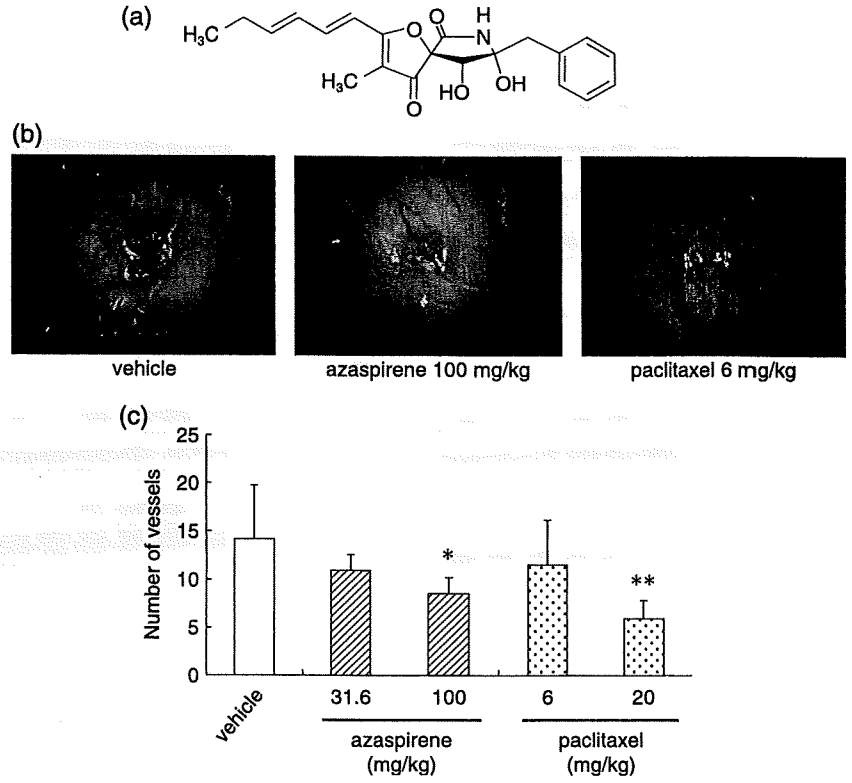

Fig. 1. Effect of azaspirene on tumor-induced angiogenesis *in vivo*. (a) The chemical structure of azaspirene. (b) Photographs of tumor-induced vessel formation after treatment with vehicle, azaspirene, and paclitaxel. (c) Quantification of newly formed blood vessels. The statistical significance of differences between the control and experimental groups was determined using one-way ANOVA, Tukey method analysis, repeated measures. $*P < 0.05$; $**P < 0.01$ was taken as the level of statistical significance.

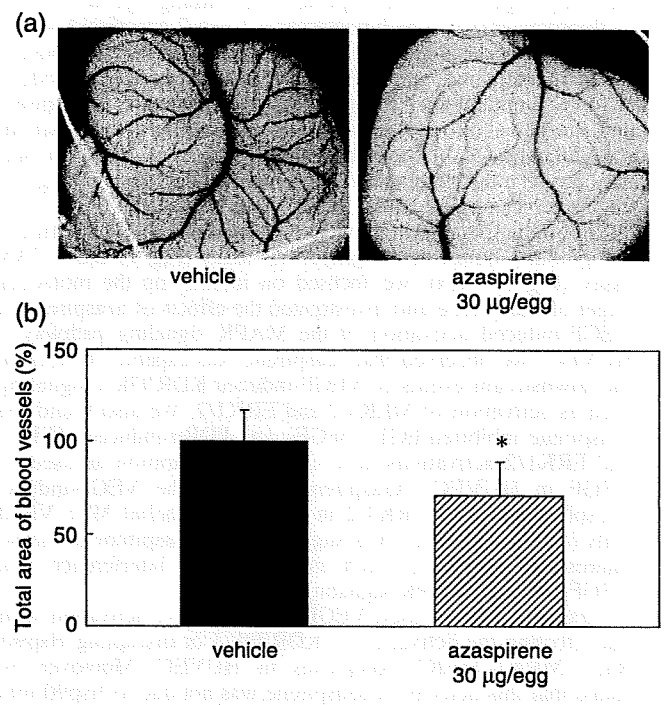

Fig. 2. Suppression of blood vessel formation within chorioallantoic membrane (CAM) by azasprirene. (a) The 4.5-day-old CAM were treated with increasing concentrations of azaspirene for 48 h, and then patterns of angiogenesis were photographed. (b) The total area of blood vessels was analyzed with angiogenesis-measuring software and is shown under each panel. Solid column, vehicle (10% dimethyl sulfoxide); hatched column, 30 μg/egg azaspirene. The statistical significance of differences between control and experimental groups was determined using two-group two-tailed Student's *t*-test. $*P < 0.05$ was taken as the level of statistical significance.

phosphorylation of Raf-1 and Raf-1-binding proteins. The results showed that azaspirene inhibited VEGF-induced phosphorylation of Raf-1 in a dose-dependent manner (Fig. 4a). Additionally, azaspirene had no effect on the disruption of Hsp90–Raf-1–MEK complexes and did not markedly suppress VEGF-induced KDR/Flk-1 autophosphorylation at concentrations up to 81 μmol/L (Fig. 4a,b). These data suggest that the mode of action of azaspirene is different from those of known antiangiogenic compounds, such as the receptor tyrosine kinase inhibitor, vatalanib, Raf-1 kinase inhibitor, and sorafenib.[13–17]

Azaspirene did not inhibit angiogenic factor-induced activation of ERK1/2 in NIH3T3, HeLa, MSS31, and MCF-7 cells. To investigate the effect of azaspirene on the activation of ERK1/2 in several cell lines other than HUVEC, we examined the phosphorylation of ERK1/2 in non-vascular endothelial cells. As shown in Fig. 5a, phosphorylation of ERK1/2 induced by bFGF, PDGF, and PDBu in NIH3T3 cells was not remarkably suppressed by azaspirene at 81 or 270 μmol/L. Similarly, azaspirene did not inhibit the phosphorylation of ERK1/2 induced by EGF or PDBu in HeLa, MSS31, or MCF-7 cells (Fig. 5b,c). These results suggest that azaspirene specifically inhibits the MAPK signaling pathway in vascular endothelial cells.

Azaspirene preferentially inhibited the growth of HUVEC and suppressed MAPK activation in HEK293T cells transiently expressing KDR/Flk-1. To investigate the effect of azaspirene on cell growth inhibition and MAPK activation in HEK293T cells transiently expressing KDR/Flk-1, we examined the unique biological activities of azaspirene on HUVEC. We first tested the effects of azaspirene on the growth of NIH3T3, HeLa, MSS31, MCF-7, and HUVEC in a proliferation assay. Interestingly, azaspirene preferentially inhibited the growth of HUVEC rather than those of the other four cell lines at 81.4 μmol/L (Fig. 6a). In addition, we investigated whether azaspirene influenced VEGF-triggered activation of the MAPK signaling pathway in HEK293T cells transiently expressing KDR/Flk-1.[33] VEGF-induced ERK1/2 activation was strongly inhibited by azaspirene at 27 μmol/L

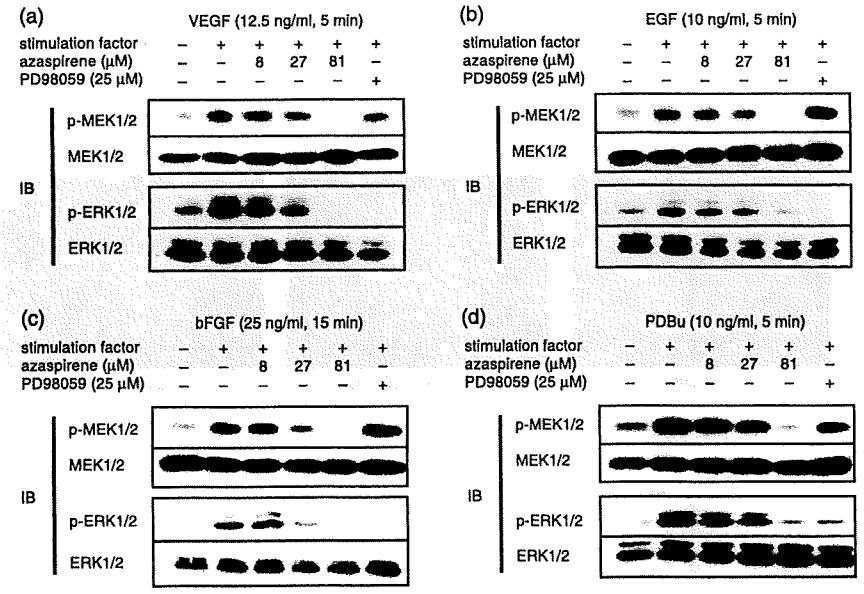

Fig. 3. Effect of azaspirene on the mitogen-activated protein (MAP) kinase signaling pathways in human umbilical vein endothelial cells (HUVEC). Azaspirene inhibited the phosphorylation of MEK1 and 2 and ERK1 and 2 induced by (a) vascular endothelial growth factor (VEGF), (b) epidermal growth factor (EGF), (c) basic fibroblast growth factor (bFGF), and (d) phorbol 12, 13-dibutyrate (PDBu). HUVEC were pretreated for 60 min with various concentrations (8, 27, or 81 μmol/L) of azaspirene and PD98059 (25 μmol/L) before exposure to VEGF (12.5 ng/mL) for 5 min, EGF (10 ng/mL) for 5 min, bFGF (25 ng/mL) for 15 min, or PDBu (10 ng/mL) for 5 min. After stimulation the cells were harvested and western blotting was carried out. IB, antibodies used for western blotting. The results shown are representative of three experiments.

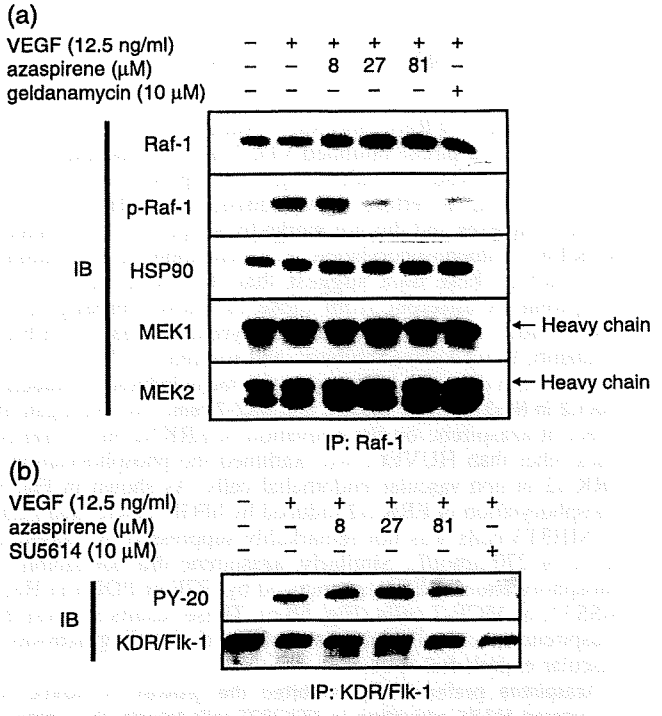

Fig. 4. Effect of azaspirene on the autophosphorylation of kinase insert domain-containing receptor/fetal liver kinase 1 (KDR/Flk-1), phosphorylation of Raf-1, and disruption of Raf-1 complexes. (a) Azaspirene did not inhibit the autophosphorylation of KDR/Flk-1 induced by vascular endothelial growth factor (VEGF). Human umbilical vein endothelial cells (HUVEC) were pretreated for 60 min with various concentrations (8, 27, or 81 μmol/L) of azaspirene and SU5614 (10 μmol/L) before exposure to VEGF (12.5 ng/mL) for 5 min. (b) Azaspirene inhibited the phosphorylation of Raf-1 induced by VEGF (12.5 ng/mL, 5 min), but did not disrupt the Raf-1, Hsp90, MEK1, or MEK2 complexes. HUVEC were pretreated for 60 min with various concentrations (8, 27, or 81 μmol/L) of azaspirene and geldanamycin (10 μmol/L) before exposure to VEGF (12.5 ng/mL) for 5 min. IB, western blotting analysis; IP, immunoprecipitation experiments. The results shown are representative of three experiments.

(Fig. 6b). These results demonstrate that azaspirene has a unique biological activity of preferentially inhibiting the growth of HUVEC and would inhibit ERK1/2 activation in cells expressing KDR/Flk-1 in a specific manner.

Discussion

Recently, Igarashi *et al.* reported the antiangiogenic activity of fluorosynerazol, which possesses a 1-oxa-7-azaspiro[4.4]non-2-ene-4,6-dione skeleton identical to azaspirene.[34] Fluorosynerazol showed an antiangiogenic effect in a CAM assay, but its mode of action was not elucidated. As both fluorosynerazol and azaspirene had the same oxo-azaspiro skeleton, we sought to reveal the molecular target of azaspirene, which appeared to inhibit only new tumor-induced blood vessel formation without having any visible effect on preexisting blood vessels (Fig. 1b).

The antiangiogenic activity of azaspirene was confirmed using both a tumor neo-angiogenesis assay (Fig. 1) and a CAM assay (Fig. 2). Next, we focused on identifying the molecular target of azaspirene and investigated the effects of azaspirene on VEGF-induced activation of the MAPK signaling pathway in HUVEC. We observed that azaspirene was capable of blocking the downstream events of VEGF-induced KDR/Flk-1 signaling, such as activation of MEK1/2 and ERK1/2. We also found that azaspirene inhibited EGF-, bFGF-, and PDBu-induced MEK1/2 and ERK1/2 activations at a similar concentration as used for VEGF in HUVEC. Azaspirene inhibited the VEGF-induced phosphorylation of ERK1/2 in mouse endothelial MS1 VEGF cells (data not shown). It is suggested that azaspirene possesses interesting properties, such as preferential interference with VEGF-induced MAPK signaling in HUVEC.

Azaspirene suppressed VEGF-induced Raf-1 activation without affecting the activation of KDR/Flk-1 or disrupting Hsp90–Raf-1–MEK1–MEK2 complexes in HUVEC. Moreover, we found that this activity of azaspirene was not due to Hsp90 inhibition (data not shown). Thus, azaspirene specifically blocked VEGF-induced phosphorylation of Raf-1, but the molecular target through which it exerts its effects remains unknown. There are controversial reports on Raf-1 activation in endothelial cells. One research group suggested Ras-independent Raf-1 activation via a protein kinase C (PKC)-dependent pathway.[29,35,36] Another group suggested the involvement of p21-activated protein kinase-1 and src kinase on Raf-1 activation.[37–39] To clarify the

doi: 10.1111/j.1349-7006.2008.00890.x

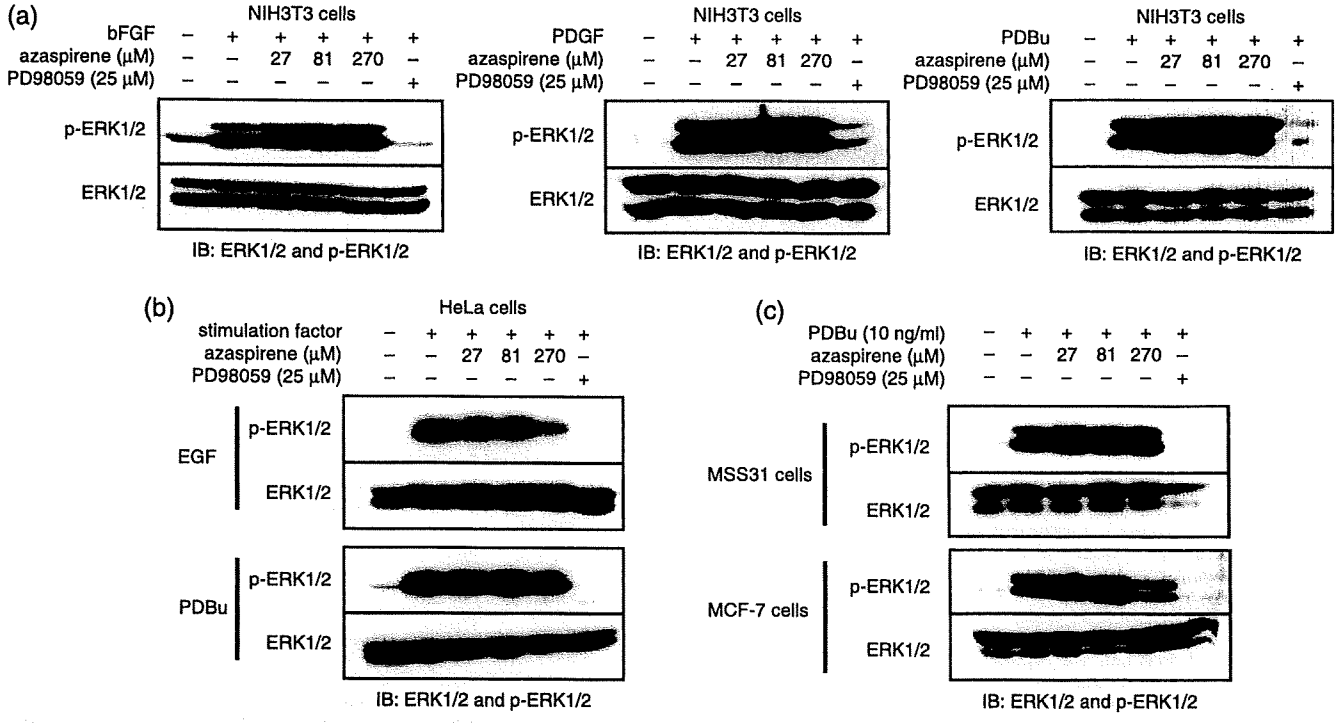

Fig. 5. Effect of azaspirene on the mitogen-activated protein (MAP) kinase signaling pathways in NIH3T3, HeLa, MSS31, and MCF-7 cells. Azaspirene did not inhibit the phosphorylation of ERK1 and 2 induced by platelet-derived growth factor (PDGF), epidermal growth factor (EGF), or phorbol 12, 13-dibutyrate (PDBu) in other cell lines. (a) NIH3T3 cells were pretreated for 60 min with various concentrations (27, 81, or 270 μmol/L) of azaspirene and PD98059 (25 μmol/L) before exposure to basic fibroblast growth factor (bFGF) (10 ng/mL) for 5 min, PDGF (30 ng/mL) for 5 min, or PDBu (10 ng/mL) for 5 min. (b) Azaspirene did not inhibit the phosphorylation of ERK1 and 2 induced by EGF (10 ng/mL, 5 min) or PDBu (10 ng/mL, 5 min) in HeLa cells. (c) MSS31 and MCF-7 cell lines were pretreated for 60 min with various concentrations (27, 81, or 270 μmol/L) of azaspirene and PD98059 (25 μmol/L) before exposure to PDBu (10 ng/mL) for 5 min. After stimulation, the cells were harvested and western blotting was carried out. IB, western blotting analysis. The results shown are representative of three experiments.

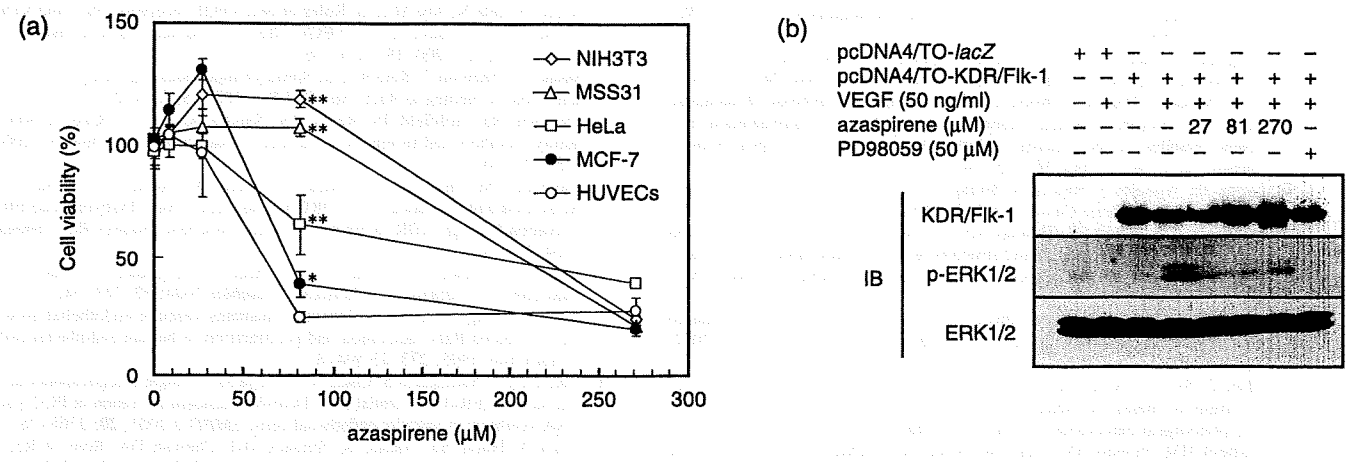

Fig. 6. Effects of azaspirene on the growth of human umbilical vein endothelial cells (HUVEC) and on mitogen-activated protein kinase (MAPK) activation in the HEK293T cell system. (a) Effects of azaspirene on the growth of NIH3T3, HeLa, MSS31, and MCF-7 cells and HUVEC in a proliferation assay. The azaspirene-induced growth inhibitions for the different cell lines were as follows: ◇, NIH3T3 (IC_{50} = 216 μmol/L); □, HeLa (IC_{50} = 189 μmol/L); △, MSS31 (IC_{50} = 173 μmol/L); ●, MCF-7 (IC_{50} = 75.6 μmol/L); and ○, HUVEC (IC_{50} = 62.1 μmol/L). Each value is expressed relative to the 1% dimethyl sulfoxide (DMSO) control group; bars, SD. The statistical significance of differences between the growth inhibition (%) of HUVEC with azaspirene at 81 μmol/L was determined using one-way ANOVA, Tukey method analysis, repeated measures. $*P < 0.05$; $**P < 0.01$ was taken as the level of statistical significance. (b) Effects of azaspirene on vascular endothelial growth factor (VEGF)-induced ERK1 and 2 phosphorylation in HEK293T cells expressing kinase insert domain-containing receptor/fetal liver kinase 1 (KDR/Flk-1). HEK293T cells transfected with KDR/Flk-1 were incubated for 1 h in the absence (DMSO) or presence of various concentrations of azaspirene (27, 81, or 270 μmol/L). These cells were then treated with 50 ng/mL VEGF for 5 min. After stimulation, the cells were harvested, and western blotting was carried out. IB, western blotting analysis. The results shown are representative of three experiments.

molecular mechanism of Raf-1 activation, we elucidated the mechanism of azaspirene.

It is noteworthy that azaspirene preferentially inhibited the cell growth of HUVEC when compared with NIH3T3, HeLa, MSS31, and MCF-7 cells (Fig. 6a). Next, we demonstrated that azaspirene inhibited the activation of ERK1/2 in KDR/Flk-1-overexpressing HEK293T cells (Fig. 6b). These results were consistent with the observation that azaspirene specifically inhibits the MAPK signaling pathway in HUVEC.

In conclusion, our current data demonstrate that azaspirene had antiangiogenic properties *in vivo*, and we have revealed that the effects of azaspirene on Raf-1 activation might be correlated with its antiangiogenic activity. Further intensive studies of the target identification of azaspirene will unravel the mystery of the VEGF-signaling pathway in HUVEC.

Acknowledgments

This work was supported in part by a Grant-in-Aid from the Ministry of Education, Culture, Sports, Science, and Technology of Japan, by a Grant-in-Aid for Cancer Research from the Ministry of Health, Labour, and Welfare of Japan, by the Chemical Biology Project (RIKEN), and by funding from the Special Postdoctoral Researchers Program (to Y. A.). The authors thank the Screening Committee of New Anticancer Agents, which is supported by a Grant-in-Aid for Scientific Research on the Priority Area 'Cancer' from The Ministry of Education, Culture, Sports, Science, and Technology of Japan. We are grateful to Ms. K. Kawai, Dr. Y. Tamura, Dr. S. Takahashi, and Dr. S. Simizu (RIKEN) for suggestions concerning the western blotting and immunoprecipitation experiments.

References

1 Bussolino F, Mantovani A, Persico G. Molecular mechanisms of blood vessel formation. *Trends Biochem Sci* 1997; **22**: 251–6.
2 Inser JM, Asahara T. Angiogenesis and vasculogenesis as therapeutic strategies for postnatal neovascularization. *J Clin Invest* 1999; **103**: 1231–6.
3 Hanhan D, Folkman J. Patterns and emerging mechanisms of the angiogenic switch during tumorigenesis. *Cell* 1996; **82**: 353–64.
4 Folkman J. What is the evidence that tumors are angiogenesis dependent? *J Natl Cancer Inst* 1990; **80**: 4–6.
5 Fidler IJ, Ellis LM. The implications of angiogenesis for the biology and therapy of cancer metastasis. *Cell* 1994; **79**: 185–8.
6 Murakami M, Iwai S, Hiratsuka S *et al.* Signaling of vascular endothelial growth factor receptor-1 tyrosine kinase promotes rheumatoid arthritis through activation of monocytes/macrophages. *Blood* 2006; **108**: 1849–56.
7 Shibuya M, Claesson-Welsh L. Signal transduction by VEGF receptors in regulation of angiogenesis and lymphangiogenesis. *Exp Cell Res* 2006; **312**: 549–60.
8 He Y, Rajantie I, Pajusola K *et al.* Vascular endothelial cell growth factor receptor 3-mediated activation of lymphatic endothelium is crucial for tumor cell entry and spread via lymphatic vessels. *Cancer Res* 2005; **65**: 4739–46.
9 Sridhar SS, Hedley D, Siu LL. Raf kinase as a target for anticancer therapeutics. *Mol Cancer Ther* 2005; **4**: 677–85.
10 Olsson AK, Dimberg A, Kreuger J, Claesson-Welsh L. VEGF receptor signalling – in control of vascular function. *Nat Rev Mol Cell Biol* 2006; **7**: 359–71.
11 Wilhelm SM, Carter C, Tang L *et al.* BAY 43-9006 exhibits broad spectrum oral antitumor activity and targets the RAF/MEK/ERK pathway and receptor tyrosine kinases involved in tumor progression and angiogenesis. *Cancer Res* 2004; **64**: 7099–109.
12 Dasgupta P, Sun J, Wang S *et al.* Disruption of the Rb–Raf-1 interaction inhibits tumor growth and angiogenesis. *Mol Cell Biol* 2004; **24**: 9527–41.
13 Xu L, Yoneda J, Herrera C, Wood J, Killion JJ, Fidler IJ. Inhibition of malignant ascites and growth of human ovarian carcinoma by oral administration of a potent inhibitor of the vascular endothelial growth factor receptor tyrosine kinases. *Int J Oncol* 2000; **16**: 445–54.
14 Lyons JF, Wilhelm S, Hibner B, Bollag G. Discovery of a novel Raf kinase inhibitor. *Endocr Relat Cancer* 2001; **3**: 219–25.
15 Hennequin LF, Stokes ES, Thomas AP *et al.* Novel 4-anilinoquinazolines with C-7 basic side chains: design and structure activity relationship of a series of potent, orally active, VEGF receptor tyrosine kinase inhibitors. *J Med Chem* 2002; **45**: 1300–12.
16 Duran I, Hotte SJ, Hirte H *et al.* Phase I targeted combination trial of sorafenib and erlotinib in patients with advanced solid tumors. *Clin Cancer Res* 2007; **13**: 4849–57.
17 Elser C, Siu LL, Winquist E *et al.* Phase II trial of sorafenib in patients with recurrent or metastatic squamous cell carcinoma of the head and neck or nasopharyngeal carcinoma. *J Clin Oncol* 2007; **25**: 3766–73.
18 Verheul HM, Pinedo HM. Possible molecular mechanisms involved in the toxicity of angiogenesis inhibition. *Nat Rev Cancer* 2007; **7**: 475–85.
19 Asami Y, Kakeya H, Onose R, Chang YH, Toi M, Osada H. RK-805, an endothelial-cell-growth inhibitor produced by *Neosartorya* sp. and a docking model with methionie aminopeptidase-2. *Tetrahedron* 2004; **60**: 7085–91.
20 Kakeya H, Onose R, Koshino H *et al.* Epoxyquinol A, a highly functionalized pentaketide dimer with antiangiogenic activity isolated from fungal metabolites. *J Am Chem Soc* 2002; **124**: 3496–7.
21 Kakeya H, Onose R, Yoshida A, Koshino H, Osada H. Epoxyquinol B, a fungal metabolite with a potent antiangiogenic activity. *J Antibiot* 2002; **55**: 829–31.
22 Kakeya H, Onose R, Koshino H, Osada H. Epoxytwinol A, a novel unique angiogenesis inhibitor with C2 symmetry, produced by a fungus. *Chem Commun* 2005; **20**: 2575–7.
23 Asami Y, Kakeya H, Okada G, Toi M, Osada H. RK-95113, a new angiogenesis inhibitor produced by *Aspergillus fumigatus*. *J Antibiot* 2006; **59**: 724–8.
24 Asami Y, Kakeya H, Onose R, Yoshida A, Matsuzaki H, Osada H. Azaspirene: a novel angiogenesis inhibitor containing a 1-oxa-7-azaspiro[4.4]non-2-ene-4,6-dione skeleton produced by the fungus *Neosartorya* sp. *Org Lett* 2002; **17**: 2845–8.
25 Kreisle R, Ershler W. Investigation of tumor angiogenesis in an id mouse model: role of host–tumor interactions. *J Natl Cancer Inst* 1988; **80**: 849–54.
26 Suzuki Y, Komi Y, Ashino H *et al.* Retinoic acid controls blood vessel formation by modulating endothelial and mural cell interaction via suppression of Tie2 signaling in vascular progenitor cells. *Blood* 2004; **104**: 166–9.
27 Simizu S, Tamura Y, Osada H. Dephosphorylation of Bcl-2 by protein phosphatase 2A results in apoptosis resistance. *Cancer Sci* 2004; **95**: 266–70.
28 Tamura Y, Simizu S, Osada H. The phosphorylation status and anti-apoptotic activity of Bcl-2 are regulated by ERK and protein phosphatase 2A on the mitochondria. *FEBS Lett* 2004; **569**: 249–55.
29 Takahashi T, Ueno H, Shibuya M. VEGF activates protein kinase C-dependent, but Ras-independent Raf–MEK–MAP kinase pathway for DNA synthesis in primary endothelial cells. *Oncogene* 1999; **18**: 2221–30.
30 Kanno S, Oda N, Abe M *et al.* Roles of two VEGF receptors, Flt-1 and KDR, in the signal transduction of VEGF effects in human vascular endothelial cells. *Oncogene* 2000; **19**: 2138–46.
31 Sasaki A, Taketomi T, Kato R *et al.* Sprouty4 suppresses Ras-independent ERK activation by binding to Raf1. *Nat Cell Biol* 2003; **5**: 427–32.
32 Tomanek RJ, Holifield JS, Reiter RS, Sandra A, Lin JJ. Role of VEGF family members and receptors in coronary vessel formation. *Dev Dyn* 2002; **225**: 233–40.
33 Kuriyama M, Taniguchi T, Shirai Y, Sasaki A, Yoshimura A, Saito N. Activation and translocation of PKCδ is necessary for VEGF-induced ERK activation through KDR in HEK293T cells. *Biochem Biophys Res Commun* 2004; **325**: 843–51.
34 Igarashi Y, Yabuta Y, Sekine A *et al.* Directed biosynthesis of fluorinated pseurotin A, synerazol and gliotoxin. *J Antibiot* 2004; **57**: 748–54.
35 Hood J, Granger HJ. Protein kinase G mediates vascular endothelial growth factor-induced Raf-1 activation and proliferation in human endothelial cells. *J Biol Chem* 1998; **273**: 23 504–8.
36 Takahashi T, Yamaguchi S, Chida K, Shibuya M. A single autophosphorylation site on KDR/Flk-1 is essential for VEGF-A-dependent activation of PLC-γ and DNA synthesis in vascular endothelial cells. *EMBO J* 2001; **20**: 2768–78.
37 Alavi A, Hood JD, Frausto R, Stupack DG, Cheresh DA. Role of Raf in vascular protection from distinct apoptotic stimuli. *Science* 2003; **301**: 94–6.
38 Hood JD, Frausto R, Kiosses WB, Schwartz MA, Cheresh DA. Differential αv integrin-mediated Ras–ERK signaling during two pathways of angiogenesis. *J Cell Biol* 2003; **162**: 933–43.
39 Chong H, Vikis HG, Guan KL. Mechanisms of regulating the Raf kinase family. *Cell Signal* 2003; **15**: 463–9.

doi: 10.1111/j.1349-7006.2008.00890.x